Journal of Medicinal Chemistry

Article

pubs.acs.org/jmc

Optimization of Sphingosine-1-phosphate-1 Receptor Agonists: Effects of Acidic, Basic, and Zwitterionic Chemotypes on Pharmacokinetic and Pharmacodynamic Profiles

John Skidmore,[§] Jag Heer,[§] Christopher N. Johnson,[§] David Norton,[§] Sally Redshaw,[§] Jennifer Sweeting,[§] David Hurst,[§] Andrew Cridland,[§] David Vesey,[§] Ian Wall,[§] Mahmood Ahmed,[‡] Dean Rivers,[‡] James Myatt,[§] Gerard Giblin,[§] Karen Philpott,[§] Umesh Kumar,[§] Alexander Stevens,[§] Rino A. Bit,[†] Andrea Haynes,[†] Simon Taylor,[†] Robert Watson,[†] Jason Witherington,[†] Emmanuel Demont,*[,†] and Tom D. Heightman*[,§]

[§]Neurology Center of Excellence for Drug Discovery, GlaxoSmithKline, New Frontiers Science Park, Harlow CM19 5AW, U.K.

[†]Immuno Inflammation Center of Excellence for Drug Discovery, GlaxoSmithKline, Gunnels Wood Road, Stevenage, SG1 2NY, U.K.

[‡]Neural Pathways DPU, GlaxoSmithKline, 11 Biopolis Way, Singapore 138667

Supporting Information

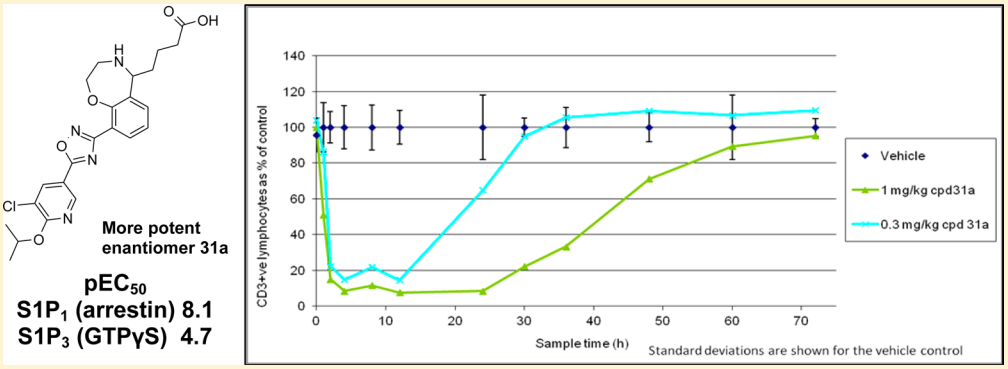

ABSTRACT: The efficacy of the recently approved drug fingolimod (FTY720) in multiple sclerosis patients results from the action of its phosphate metabolite on sphingosine-1-phosphate $S1P_1$ receptors, while a variety of side effects have been ascribed to its $S1P_3$ receptor activity. Although S1P and phospho-fingolimod share the same structural elements of a zwitterionic headgroup and lipophilic tail, a variety of chemotypes have been found to show $S1P_1$ receptor agonism. Here we describe a study of the tolerance of the $S1P_1$ and $S1P_3$ receptors toward bicyclic heterocycles of systematically varied shape and connectivity incorporating acidic, basic, or zwitterionic headgroups. We compare their physicochemical properties, their performance in *in vitro* and *in vivo* pharmacokinetic models, and their efficacy in peripheral lymphocyte lowering. The campaign resulted in the identification of several potent $S1P_1$ receptor agonists with good selectivity vs $S1P_3$ receptors, efficacy at <1 mg/kg oral doses, and developability properties suitable for progression into preclinical development.

INTRODUCTION

The recent FDA approval of fingolimod (**1a**, Figure 1) has provided a novel mechanism of treatment for patients suffering from relapsing−remitting multiple sclerosis.[1] In preclinical species and in patients, administration of fingolimod elicits the sequestration of lymphocytes in secondary lymphoid organs, resulting in a reduction in the count of circulating peripheral lymphocytes and a concomitant amelioration in the frequency and severity of autoimmune-mediated neuroinflammatory lesions.[2,3] Fingolimod is an aminodiol and is phosphorylated enantioselectively *in vivo* by sphingosine kinase-2.[4,5] The resulting phosphate (**1b**) mimics the endogenous agonist sphingosine-1-phosphate (S1P, **2**), displaying agonist activity at $S1P_1$ and $S1P_{3-5}$ G-protein coupled receptor subtypes.[6] A significant body of evidence indicates that the action of fingolimod and other small molecule agonists on the $S1P_1$ receptor alone is both necessary and sufficient to elicit effects on lymphocyte localization.[7−9]

Although fingolimod is generally well tolerated, a variety of adverse events have been noted, some of which were ascribed to activity on $S1P_{3-5}$ receptors.[10] Transient bradycardia is noted in both patients and rodents after the first dose of fingolimod: studies in rodents showed this effect to be primarily mediated by action on $S1P_3$ receptors,[11,12] but subsequently the $S1P_{1/5}$ agonist BAF312 was also shown to affect heart rate in

Received: August 19, 2014

   dx.doi.org/10.1021/jm5010336 | *J. Med. Chem.* XXXX, XXX, XXX−XXX

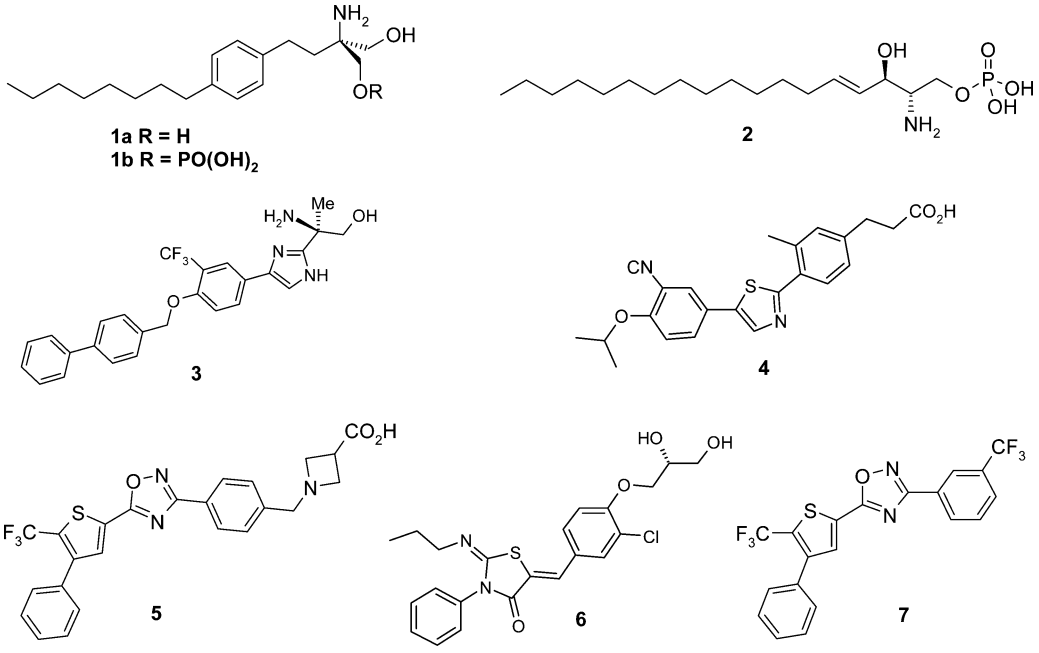

Figure 1. Selected examples of published $S1P_1$ receptor agonists or prodrugs thereof.

Table 1. S1P Receptor Activity and in Vitro Developability Properties of Heteroaryl-based Carboxylic Acids

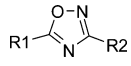

Compound	R1	R2	pEC_{50} (n, GTPγS assay) $S1P_1$	pEC_{50} (n, GTPγS assay) $S1P_3$	clogP	Fub % (HSA)
8	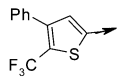	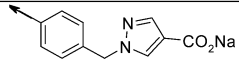	6.6 (352)	5.8 (148)	6.29	1.0-1.8
9	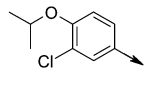	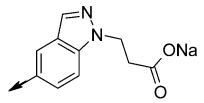	7.5 (32)	< 4.5 (14)	4.36	1.3-2.5
10	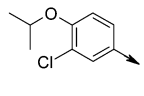	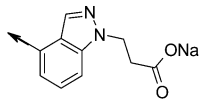	7.7 (86)	<4.5 (89)	4.36	1.2-1.3

healthy subjects despite being devoid of $S1P_3$ receptor agonism,[13] highlighting a species difference in S1P receptor subtype function. Other fingolimod dose-related adverse events include macular edema, modest hypertension, and pulmonary effects including cough and dyspnea, the latter two being ascribed to action on smooth muscle $S1P_3$ receptors.[10] Together, these observations have spurred the quest for compounds showing selective agonism of $S1P_1$ receptors since this profile appears most likely to show a favorable balance of efficacy vs adverse events.

Although both S1P and phospho-fingolimod share the same structural elements of a zwitterionic headgroup and lipophilic tail, an impressive diversity of chemotypes have been found to show S1P receptor agonism, revealing a relatively tolerant pharmacophore and a rich opportunity for medicinal chemists, as reviewed recently.[14] Example approaches include alternative scaffolds bearing hydroxy groups that undergo *in vivo* phosphorylation such as **3**[15] (Figure 1), generating a zwitterionic species with S1P receptor activity, and a variety of scaffolds that act as direct agonists without the need for *in vivo* activation, mimicking the lipophilic tail of S1P together with a negatively charged (**4**),[16] zwitterionic (**5**),[17] or uncharged polar headgroup (**6**),[18] or even with no polar headgroup, such as **7**.[17]

Encouraged by the emerging preclinical and clinical data supporting the use of $S1P_1$ agonists as therapeutic agents for the treatment of multiple sclerosis and by the above-described pharmacophore tolerance, we were motivated to seek a high quality clinical candidate with a PK/PD profile suitable for once-daily dosing in man and physicochemical properties likely to minimize attrition arising from safety and tolerability issues. First, we aimed for high selectivity for $S1P_1$ over $S1P_3$ receptors to minimize the cardiovascular side effects observed with fingolimod, as discussed above. Second, although to date fingolimod appears reasonably well-tolerated,[19] its long clinical half-life (6−9 days)[20] could cause difficulties in case of the need to rapidly withdraw treatment; hence, we specifically sought compounds likely to show reversibility within 24 h. Third, we sought to balance on-target activity with favorable molecular weight and lipophilicity, to reduce protein binding and nonspecific binding properties (drug efficiency index),[21] and to minimize the risk of preclinical or clinical toxicity.[22,23] This

dx.doi.org/10.1021/jm5010336 | J. Med. Chem. XXXX, XXX, XXX−XXX

report describes our approach to exploring the tolerance of the $S1P_1$ pharmacophore toward acidic, basic, and zwitterionic compounds, and a comparison of their properties in *in vitro* and *in vivo* pharmacokinetic, pharmacodynamic, and safety models.

RESULTS AND DISCUSSION

Carboxylic Acids. In the course of recent work targeting selective antagonists of the prostaglandin-E receptor EP1, we noted that pyrazole carboxylic acids showed promising oral exposure *in vivo*.[24] Several groups have demonstrated the favorable $S1P_1$ activity and pharmacokinetic properties of the 3,5-disubstituted oxadiazoles,[16,17,25] and merging these chemotypes led to the design of **8** (Table 1) in which a 1,2,4-oxadiazole is substituted on *C*-3 with 1-phenyl-1*H*-pyrazole-3-carboxylic acid and on *C*-5 with a thiophene bearing lipophilic substituents. This compound shows moderate $S1P_1$ receptor affinity, acting as a full agonist with a pEC_{50} of 6.6 in the GTPγS assay, albeit with modest 8-fold selectivity over the $S1P_3$ receptor (pEC_{50} of 5.8), and was therefore progressed to the lymphopenia model in rats, as described previously.[26] Significant lymphocyte lowering was observed after a 3 mg/kg oral dose, and persisted over 48 h. PK sampling confirmed that this prolonged PD response was driven by high systemic levels of **8** (2.4 μM at the 48 h time point). The prolonged exposure is presumably a consequence of high plasma protein binding (HSA F_{ub} 0.4%, based on chromatographic measurement[27]), and possibly enterohepatic recirculation, a common feature of lipophilic acids.[28]

We next sought to identify compounds with reduced lipophilicity, in order to diminish the extent of plasma protein binding, hoping thereby to reduce the prolonged PK half-life and elicit maximal lymphopenia at lower total plasma concentrations. First, we replaced the highly lipophilic trifluoromethyl substituted thiophene with a 3-chloro-4-isopropoxyphenyl group[29] and explored the effects of merging the phenyl and pyrazole rings into a series of bicyclic cores (Table 1), an approach also pursued by others.[30] In this series, both ethylene- and propylene-linked indazole carboxylic acids showed promising potency; the best activity at $S1P_1$ and selectivity over $S1P_3$ receptors was observed in the 4-linked indazoles, represented by indazole propionic acid **10**. The properties of **10** are summarized in Table 2. As expected for a lipophilic acid, some inhibition of CYP2C9 is observed, with high plasma protein binding (>99%) across species. Metabolic stability in microsomal preparations is good, while permeability in MDCK cells is modest. As expected the solubility of **10** is pH dependent, being below quantifiable levels in simulated gastric fluid (SGF) but reaching 44 μg/mL in fed-state simulated intestinal fluid (FeSSIF).[31] Despite this limited solubility, **10** has a superior profile in the rat lymphopenia model compared with **8**: maximal lowering of lymphocyte levels was achieved following a 1 mg/kg oral dose, and *in vivo* IC_{50} of 117 nM was calculated from PK sampling across the doses.[32] Importantly, the lymphopenia was found to be reversible within 24 h even after repeat dosing for 7 days (Figure 2a,b). Moreover, indazole acid **10** shows promising pharmacokinetic properties across species: oral bioavailability values range from 59% to 96% in rats, dogs, and cynomolgus monkeys, with half-lives in the range 1.0−7.6 h, albeit with low volume of distribution generally associated with acidic molecules.[33]

Basic Heterocycles. We next replaced the heteroaryl pyrazole core with fused aromatic−aliphatic systems that would introduce a basic center to explore effects on plasma protein binding, tissue distribution, and solubility. We based these molecules on the 5-(4-isopropoxyphenyl)-1,2,4-oxadiazole unit, substituted *ortho*- to the isopropoxy substituent with either a nitrile or a chloride, which had delivered good agonist activity in the indazole series. We systematically introduced regioisomers of phenyl-fused five-, six-, and seven-membered

Table 2. *In Vitro* and *in Vivo* Properties of Indazole Propionic Acid 10

MW, PSA, cLogP		427, 103, 4.36
CHI log *D* @ pH 2.0, 7.4, and 10.5		4.11, 2.26,1.83
$S1P_1$ pEC_{50} (*n*, GTPγS)		7.7 (86)
$S1P_3$ pEC_{50} (*n*, GTPγS)		<4.5 (89)
solubility @ 24 h (mg/mL)	SGF (pH 1.2)	not detected
	FeSSIF (pH 5)	0.044
	FASSIF (pH 6.5)	0.011
CYP IC_{50} (μM,; 1A2, 2C9, 2C19, 2D6, 3A4VG, 3A4VR, *n* = 2−4)		>50, 7 ± 0.8, >50, >50, 28 ± 19, 25 ± 13
permeability (MDCK type 2, nm/s)		203
Fu blood (rat, dog, cyno, human)		0.0017, 0.0020, 0.0018, 0.0010
hepatocyte CLi (mL/(min·g); rat, dog, cyno, human)		<0.9, <1.7, 0.9, <0.9
in vivo IC_{50} (nM)		117
rat PK (1 mg/kg iv[a] or 3 mg/kg po;[b] *n* = 3)	CLb (mL/(min·kg))[a]	2 ± 0
	Vss (L/kg)[a]	1.0 ± 0.1
	$t_{1/2}$ (iv, h)[a]	7.5 ± 0.4
	F, po, %[b]	96 ± 16
dog PK (1 mg/kg iv[a] or 2 mg/kg po;[b] *n* = 3)	CLb (mL/(min·kg))[a]	4 ± 1
	Vss (L/kg)[a]	1.0 ± 0.2
	$t_{1/2}$ (iv, h)[a]	3.9 ± 0.8
	F, po, %[b]	94 ± 3
cyno PK (1 mg/kg iv[a] or 3 mg/kg po;[b] *n* = 3)	CLb (mL/(min·kg))[a]	3 ± 0.2
	Vss (L/kg)[a]	0.4 ± 0.0
	$t_{1/2}$ (iv, h)[a]	1.2 ± 0.2
	F, po, %[b]	59 ± 18

[a]DMSO/10%(w/v) Kleptose, 0.9% saline(aq) (2%/98%). [b]Methylcellulose(aq), 1% (w/v), po suspension.

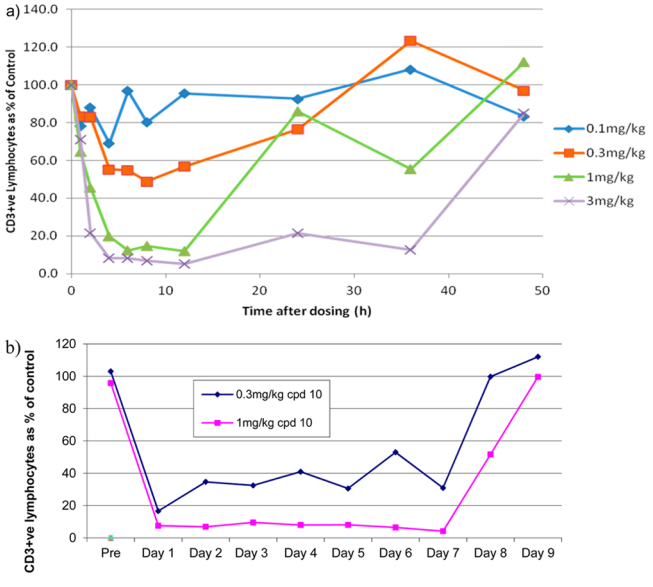

Figure 2. Effects of indazole propionic acid **10** on circulating lymphocyte levels in rats after (a) single dose in the range 0.1−3 mg/kg or (b) 7-day repeat dosing at 0.3 and 1 mg/kg, showing reversal within 24 h after the final dose.

dx.doi.org/10.1021/jm5010336 | J. Med. Chem. XXXX, XXX, XXX−XXX

Table 3. $S1P_{1/3}$ Receptor Activities for Phenyl-Fused Basic Heterocycles

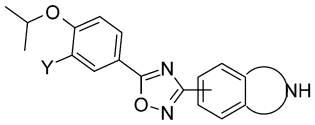

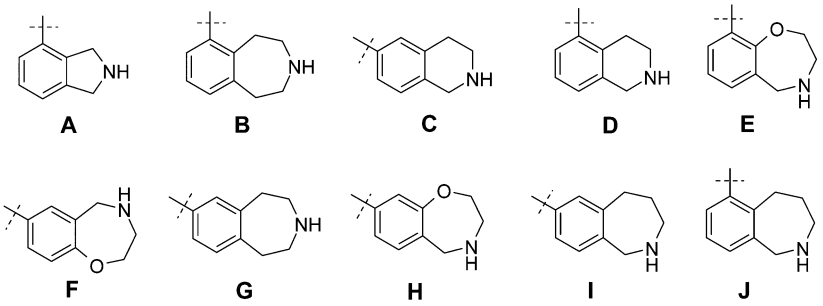

		pEC_{50} (n, GTPγS assay)[a]			
		$S1P_1$		$S1P_3$	
compound	core heterocycle	Y = Cl	Y = CN	Y = Cl	Y = CN
11a	A	8.1 (10)		<4.5 (9)	
12a,b	B	7.8 (8)	8.7 (15)	<4.5 (8)	5.1 (1/10)
13b	C		8.4 (2)		4.5 (3/4)
14a	D	7.4 (11)		4.8 (6/12)	
15a	E	7.1 (4)		<4.5 (4)	
16a,b	F	6.9 (4)	7.6 (4)	4.8 (3/4)	5.2 (4)
17a,b	G	6.8 (13)	7.6 (17)	<4.5 (6)	<4.5 (10)
18a,b	H	6.5 (7)	7.1 (4)	<4.5 (4)	<4.5 (4)
19a,b	I	6.4 (8)	6.9 (11)	<4.5 (6)	<4.5 (8)
20a	J	6.2 (4)		<4.5 (2)	

[a]In parentheses is the number of test occasions out of all tests when a pEC_{50} was obtained; otherwise the value was <4.5.

basic heterocycles, as summarized in Table 3. These compounds were found to have a range of activities at the $S1P_1$ receptor even when lacking the alkyl-carboxylate headgroup previously present in the aromatic heterocyclic series. The highest activities (pEC_{50} > 8) were observed with isoindoline **11a**, benzazepines **12a,b**, and tetrahydroisoquinoline **13b**. The tetrahydroisoquinoline isomer **14a**, the benzoxazepine isomers **15a** and **16a,b** and the benzazepine isomers **17a,b** showed intermediate potency, while the benzoxazepine isomers **18a,b** and benzazepine isomers **19a,b** and **20a** showed the lowest levels of activity (pEC_{50} < 7), although still at submicromolar levels. All these compounds showed excellent selectivity for $S1P_1$ over $S1P_3$ receptors. Interestingly, where comparisons were made, all compounds containing the *ortho*-nitrile substituent showed significantly greater potency than the corresponding *ortho*-chloro analogues. The use of aromatic nitrile as a chloride isostere in medicinal chemistry[34] and the benefits of the nitrile functionality[35] have been reviewed recently. As might be expected, *in vivo* these basic derivatives showed very different pharmacokinetic behavior to their acidic counterparts, as exemplified by the benzazepines **17a** and **17b** (Table 4). In particular, significantly higher volumes of distribution were observed, offsetting the higher clearance to give relatively long half-lives in rodents. Interestingly, despite this difference in volume of distribution, compounds from this series showed similar pharmacodynamic profiles to indazole acid **10**, as exemplified by the data for **17b** (Table 4): as for **10**, **17b** exhibited maximal lowering of lymphocyte levels following a 1 mg/kg oral dose, which was found to be reversible within 24 h.

Table 4. Pharmacokinetic and Pharmacodynamic Parameters for Benzazepines 17a and 17b Following Oral Dosing

		17a	**17b**
mouse PK (n = 3)	CLb (mL/(min·kg))[a]	10.9	18.8
	Vss (L/kg)[a]	7.6	9.1
	$t_{1/2}$ (h)[a]	9.5	6.9
	F[b], po, (%)	59	63
rat % lymphopenia at time point[c]	4 h		75
	8 h		82
	24 h		6

[a]Dose of 1 mg/kg iv DMSO/1% methylcellulose 1:99 (w/v). [b]Dose of 3 mg/kg po. For **17a**, DMSO/1% (w/v) methylcellulose 1:99. For **17b**, 1% (w/v) methylcellulose. [c]Following 1 mg/kg oral dose.

Zwitterions. Next, we explored the effect of introducing carboxyalkyl groups of varying length to the ring nitrogen of the more active basic heterocycles described above, generating zwitterions that mimic both the amino and phosphate moieties of S1P and phospho-fingolimod. Data are summarized in Table 5. In this form, compounds containing the 4-substituted isoindoline (**21a−c**), 6-linked benzazepine (**22a,b**), and benzoxazepine (**23a−c**) gave only moderate potencies ($S1P_1$ GTPγS pEC_{50} 5.6−7.3), regardless of the length of the carboxyalkyl chain. We surmised that the L-shape imposed on these compounds by cores A, B, and F is less well tolerated by the $S1P_1$ receptor. Better results were achieved with the 5- and 6-linked isoquinoline cores in **24a** and **25a** and 7-linked benzazepine in **27a−c**, which can adopt a more linear

dx.doi.org/10.1021/jm5010336 | J. Med. Chem. XXXX, XXX, XXX−XXX

Table 5. $S1P_{1/3}$ Receptor Activities for Phenyl-Fused Basic Heterocycles Bearing an N-Linked Carboxyalkyl Group

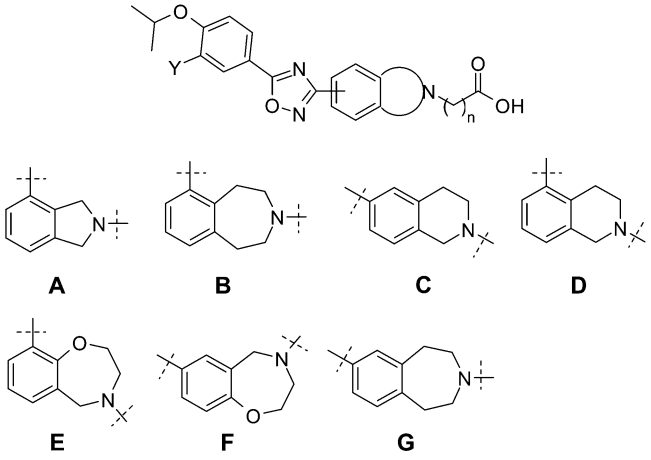

				pEC_{50} $(n)^a$ (GTPγS)	
compound	core heterocycle	n	Y	$S1P_1$	$S1P_3$
21a	A	2	Cl	6.5 (4)	5.1 (3/6)
21b		3	Cl	6.3 (4)	5.7 (5/7)
21c		3	CN	6.4 (4)	<4.5 (4)
22a	B	2	Cl	6.8 (4)	<4.5 (4)
22b		1	Cl	5.6 (2)	<4.5 (4)
23a	F	2	Cl	6.9 (6)	5.7 (1/6)
23b		2	CN	7.3 (8)	<4.5 (7)
23c		3	CN	7.2 (6)	4.6 (1/6)
24a	C	2	CN	8.2 (11)	5.4 (11)
25a	D	1	CN	8.1 (6)	<4.5 (5)
26a	E	3	Cl	7.4 (19)	<4.5 (10)
27a	G	1	CN	8.4 (16)	5.7 (5/12)
27b		2	Cl	8.1 (11)	5.0 (7/9)
27c		3	CN	8.1 (44)	5.1 (34/45)

[a]In parentheses, the number of test occasions out of all tests when a pEC_{50} was obtained; otherwise the value was <4.5.

conformation, and in this context, the *N*-acetic, -propanoic, and -butanoic acid analogues all showed similar $S1P_1$ agonist activity with pEC_{50} values >8. The 9-linked benzoxazepine **26a** showed intermediate potency. Notably, for the benzazepines **27a–c**, introduction of the carboxyalkyl group introduced weak but measurable $S1P_3$ activity, which was not observed for the smaller fused-ring derivatives. Similar derivatization of templates H and I (which had shown inferior activity in the basic heterocycle series) did not lead to improved activity (data not shown).

Having noted that an L-shape is unfavorable for the $S1P_1$ receptor activity of 4-substituted isoindoline (**21a–c**), 6-linked benzazepine (**22a,b**) and benzoxazepine (**23a–c**), we also explored the introduction of C-linked carboxyalkyl substituents to produce molecules based on these templates that lacked the unfavorable L-shape. Initially we explored the 1-substituted tetrahydroisoquinoline system bearing the oxadiazole ring on *C*-5: in this template with an acetic acid headgroup both the chloro (**28a**) and nitrile (**28b**) compounds were found to have good potency against $S1P_1$ and selectivity over $S1P_3$ (Table 6). A consequence of this structural change is the incorporation of an additional hydrogen bond donor and a concomitant reduction in lipophilicity (clogP is predicted to drop by 0.5, Daylight calculation). In addition, a chiral center is introduced, which might be expected to reduce the planarity of the compounds and could thereby improve solubility.[36]

Extending this approach to the isoindoline and benzazepine templates A and B proved synthetically challenging, but we did identify efficient routes to the benzoxazepine templates (Table 6). Interestingly, the benzoxazepines **29a,b** delivered high $S1P_1$ receptor potency, but $S1P_3$ receptor agonist activity also increased such that selectivity dropped to ∼100-fold. By contrast, the THIQs **28a,b** and benzoxazepines **30a,b** and **31a,b** showed both $S1P_1$ potency and selectivity against $S1P_3$ receptors. These findings are consistent with the structure-based observation that the $S1P_1$ receptor is more tolerant to steric hindrance than the $S1P_3$ receptor;[37] the substitution

Table 6. $S1P_{1/3}$ Receptor Activities for Phenyl-Fused Basic Heterocycles Bearing a C-Linked Carboxyalkyl Group

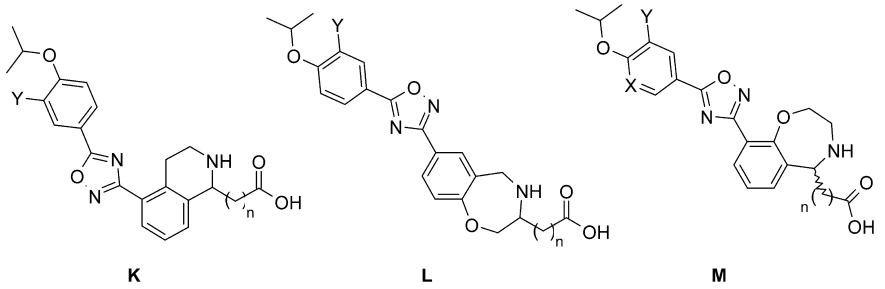

					pEC_{50} $(n)^a$ (GTPγS)	
compound	structure	n	Y	X	$S1P_1$	$S1P_3$
28a	K	1	Cl		7.7 (25)	5.3 (16/20)
28b	K	1	CN		8.3(11)	4.9 (8/12)
29a	L	0	Cl		8.3 (11)	6.1 (5/8)
29b	L	2	Cl		8.6 (12)	6.6 (6)
30a	M	2	Cl	CH	8.3 (2)	<4.5 (2)
30b	M	3	Cl	CH	8.0 (4)	4.6 (1/3)
31a[b]	M	3	Cl	N	7.4 (2)	4.7 (2/6)
31b[b]	M	3	Cl	N	7.3 (12)	5.0 (12)

[a]In parentheses, the number of test occasions out of all tests when a pEC_{50} was obtained; otherwise the value was <4.5. [b]Compounds **31a,b** are enantiomers.

dx.doi.org/10.1021/jm5010336 | J. Med. Chem. XXXX, XXX, XXX–XXX

pattern of the benzoxazepines **29a,b** leads to a relatively linear overall shape, while the THIQ (**28a,b**) or benzoxazepines (**30a,b** and **31a,b**) possess a more step-like shape with increased steric bulk between the acid and oxadiazole groups, as illustrated by the low energy conformations of **29b** vs **30a** shown in Figure 3.

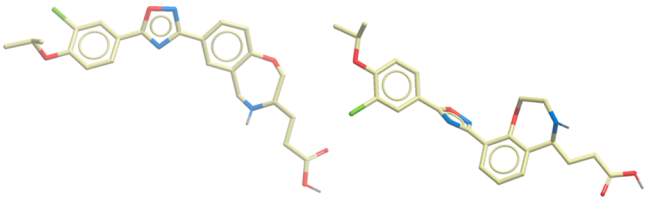

Figure 3. Three-dimensional rendering highlighting difference in overall shape of different templates represented by benzoxazepines **29b** ("linear") and **30a** ("stepped").

These investigations identified a number of zwitterionic $S1P_1$ agonists, containing either C- or N-linked carboxyalkyl groups, with promising *in vitro* activity and selectivity profiles, which were progressed to *in vivo* studies. Initially we profiled the pair of closely related compounds **28a** and **28b**, both based on a 6-aryl-substituted tetrahydroisoquinoline scaffold, differing in the nature of the substituent *ortho* to the isopropoxy group on the terminal aryl ring. While **28b**, possessing the *ortho*-nitrile, has the higher *in vitro* potency, it showed only moderate lymphopenia in the rat following a 1 mg/kg oral dose (Table 7). This result was rationalized by the associated pharmacokinetic data; the blood concentration of **28b** peaked at only 16 nM at the 4 h time point. In contrast *ortho*-chloride **28a** proved effective in the rat lymphopenia assay following a 1 mg/kg oral dose despite possessing inferior *in vitro* potency. This result is consistent with the improved pharmacokinetic properties of **28a**, which showed a peak concentration of 120 nM at 4 h.

The superior *in vivo* profile of the chloro-substituted **28a** over its nitrile counterpart **28b** proved to be representative of a general phenomenon in the zwitterionic series, with chloro-analogues showing increased exposure over the corresponding nitriles on a number of occasions (data not shown). Several parameters could account for this trend: first the chloro−nitrile switch elicits a decrease in lipophilicity (chromatographic log *D*[38] difference of ca. 0.5 units between **28a** and **28b**, see Table 7), which could influence permeability or interaction with transporters present in the gut;[39] alternatively, the chloro−nitrile switch might adversely affect solubility, which could compromise oral absorption.

Mindful of the importance of keeping a balance between a high enough log *D* to ensure effective absorption while maintaining acceptable levels of solubility, we profiled further compounds of similar chromatographic log *D* to **28a** (CHI log *D* 2.02). Compound **26a** based on the "stepped" N-linked benzoxazepine template (CHI log *D* 2.39) was profiled in the rat lymphopenia assay at 0.1, 0.3, 1, and 3 mg/kg. At the 3 mg/kg dose, **26a** caused a reduction of lymphocyte count to <20% of control levels between 2 and 12 h before returning to baseline levels at 24 h. At a 1 mg/kg dose, **26a** was only marginally less effective, whereas at doses lower than this the compound showed little or no effects in the assay (Figure 4). The *in vivo* IC_{50} based on PK sampling was calculated at 127 nM.

Table 7. Comparison of Lymphopenia and Oral Exposures for Cl- and CN-Substituted Tetrahydroquinonlines 28a and 28b

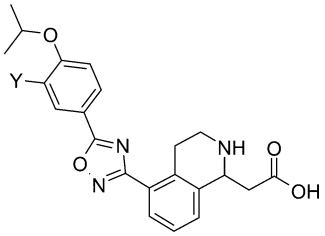

28a Y = Cl
28b Y = CN

		28a	**28b**
MW, PSA, cLogP		427, 97, 2.05	418, 121, 1.19
CHI log *D* @ pH 2.0, 7.4, and 10.5		1.47; 2.02; 1.73	1.17; 1.58; 1.27
$S1P_1$ pEC_{50} (*n*) $(GTP\gamma S)^a$		7.7 (25)	8.3 (11)
$S1P_3$ pEC_{50} (*n*) $(GTP\gamma S)^a$		5.3 (16/20)	4.9 (8/12)
lymphocyte count @ 0, 4, 8, 12, 24 h^b		99, 24, 12, 58, 99	105, 46, 69, 108, 132
[blood] @ 0, 4, 8, 12, 24 h^b (μM)		NQ, 0.120 ± 0.016, 0.086 ± 0.022, NQ, NQ	NQ, 0.016, NQ, NQ, NQ
rat PK, **28a** (1 mg/kg iv[c] or 3 mg/kg po;[d] *n* = 1)	CLb (mL/(min·kg))[d]	5	
	Vss (L/kg)[d]	2.7	
	$t_{1/2}$ (iv, h)[d]	6.7	
	F, po, %[d]	10, 18	

[a]In parentheses, the number of test occasions out of all tests when a pEC_{50} was obtained; otherwise the value was <4.5. [b]1 mg/kg po. [c]*n* = 1; DMSO/10% (w/v) Kleptose, 0.9% saline(aq) (5%/95% v/v). [d]*n* = 2; 1% (w/v) methylcelluslose(aq) po suspension.

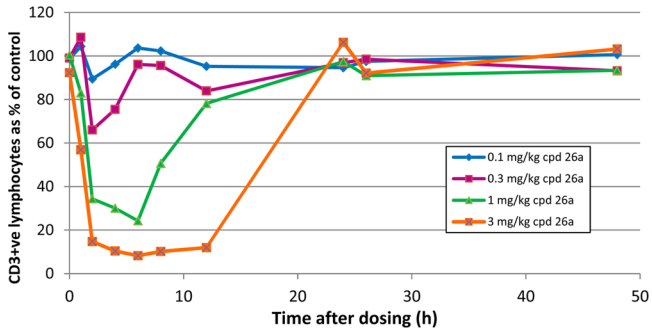

Figure 4. CD3+ lymphocyte counts in rat blood after oral dose with benzoxazepine **26a** (0.1−3 mg/kg).

Further profiling of **26a** was undertaken to explore its developability profile (Table 8). IC_{50} values against a panel of CYP450 enzymes were all greater than 26 μM. Consistent with the presence of the carboxylate functionality, **26a** was found to have a relatively low free fraction in blood; values from a range of species were <2.5%. Intrinsic clearance, determined in hepatocytes, was low in rats and in man but moderate in dogs and cynomolgus monkeys. Compound **26a** was also found to have moderate permeability across a layer of MDCK cells.[40] Consistent with these *in vitro* data, **26a** showed low clearance following a 1 mg/kg iv dose in rats and excellent bioavailability when dosed orally at 3 mg/kg. In line with the higher *in vitro* clearance values in dog and cynomolgus monkey, the *in vivo* clearance following a 1 mg iv dose was somewhat higher resulting in lower bioavailabilities in both species after a 3 mg/

dx.doi.org/10.1021/jm5010336 | J. Med. Chem. XXXX, XXX, XXX−XXX

Table 8. Selected *in Vitro* and *in Vivo* Properties of Zwitterionic Benzazepines and Benzoxazepines

properties		26a	27c	31a	31b
MW, PSA, cLogP		472, 98, 1.74	460, 112, 2.27	473, 120, 1.59	
CHI log *D* @ pH 2.0, 7.4 and 10.5		2.39[f]	1.26, 1.78, 1.50	1.02, 1.74, 1.57	
$S1P_1$ pEC_{50} (*n*) (GTPγS)		7.4 (19)	8.1 (44)	7.4 (2)	7.3 (12)
$S1P_3$ pEC_{50} (*n*) (GTPγS)		<4.5 (10)	5.1 (34/45)	4.7 (2/6)	5.0 (12)
solubility @ 24 h (mg/mL)	SGF (pH 1.2)	>1.32	0.02		
	FeSSIF (pH 5)	0.03−0.05	0.10		
	FASSIF (pH 6.5)	0.32−1.20	0.03		
pK_a amine		7.39	9.15	7.98	8.09
CYP IC_{50} (μM; 1A2, 2C9, 2C19, 2D6, 3A4VG, 3A4VR, *n* = 2−4)		>50, 27 ± 7, >50, > 50, 40 ± 14, 39 ± 16	>50, >50, >50, >50, >50, 43 ± 7	all > 50	all > 50
permeability (MDCK type 2, nm/s)		155	155		
Fu blood (rat, dog, human)		0.012, 0.018, 0.02		0.004, 0.010, 0.014	0.004, 0.015, 0.016
hepatocyte CLi (mL/(min·g); rat, dog, cyno, human)		1.0, 8.3, 4.2, 1.3	<0.85, <1.70, <0.85, <0.85	<0.9, 4, <0.9, <0.9	<0.9, 1.7, <0.9, <0.9
in vivo IC_{50} (nM)		127	15	91	99
rat PK (1 mg/kg iv[a] or 3 mg/kg po;[b] *n* = 2−3)	CLb (mL/(min·kg))[a]	7 ± 1	7 ± 1	1.03	0.71
	Vss (L/kg)[a]	1.2 ± 0.2	1.5 ± 0.21	0.6	0.4
	$t_{1/2}$ (iv, h)[a]	3.0 ± 0.7	2.6 ± 0.3	6.4	6.6
	F, po, %[b]	83 ± 16	62 ± 13	87 ± 39	78 ± 12
dog PK (1 mg/kg iv[c] and 1[e] or 2[d] mg/kg po;[c] *n* = 2−3)	CLb (mL/(min·kg))[c]	26 ± 4	3 ± 0	26	6
	Vss (L/kg)[c]	1.0 ± 1	1.6 ± 0.1	1.5	0.9
	$t_{1/2}$ (iv, h)[c]	0.4 ± 0.1	8.0 ± 2.0	0.84	1.8
	F, po, %[d,e]	57 ± 6[d]	69 ± 11[d]	50[e]	67[e]
cyno PK (1 mg/kg iv[a] or 3 mg/kg po;[c] *n* = 3)	CLb (mL/(min·kg))[b]	30 ± 2			
	Vss (L/kg)[b]	4.0 ± 1.1			
	$t_{1/2}$ (iv, h)[b]	3.2 ± 1.1			
	F, po, %[c]	39 ± 19			

[a]**26a** and **27c**, DMSO/10% (w/v) Kleptose, 0.9% saline (aq) (2%/98% v/v); **31a,b**, DMSO/10% (w/v) Kleptose HPB, 0.9% saline (aq) (5%/95% v/v). [b]**26a**, **27c**, and **31a,b**, 1% (w/v) methylcellulose (aq) po suspension. [c]**26a** and **27c**, DMSO/10% (w/v) Kleptose, 0.9% saline (aq) (2%/98% v/v); **31a,b**, DMSO/10% (w/v) Kleptose HPB, 0.9% saline (aq) (2%/98% v/v). [d]**26a** and **27c**, 1% (w/v) methylcellulose (aq). [e]**31a,b**, 1% (w/v) methylcellulose 400 (aq). [f]Determined only at pH 7.4.

kg oral dose. Based on this good correlation and the data obtained in the three different species, this compound was predicted to have a good pharmacokinetic profile in man (data not shown).

Overall it was felt that the profile of **26a** showed excellent promise from a development perspective. One remaining concern with this compound was its limited solubility: for example, solubility in fasted-state simulated intestinal fluid (FaSSIF) (pH 6.5) was found to be only 0.03−0.05 mg/mL although higher solubility was seen in both SGF and FeSSIF.[31] We had hoped that the presence of the seven-membered ring adjacent to the oxadiazole ring might reduce the planarity of compounds in the benzoxazepine series; however, as can be seen from a small molecule X-ray crystal structure of **26a**, this arrangement of rings still adopts a predominantly planar conformation, with torsion angles between the rings of only 4.9° and 7.1° (Figure 5).

Since the cyano group frequently delivered superior *in vitro* potency compared with the chloride, we also explored whether

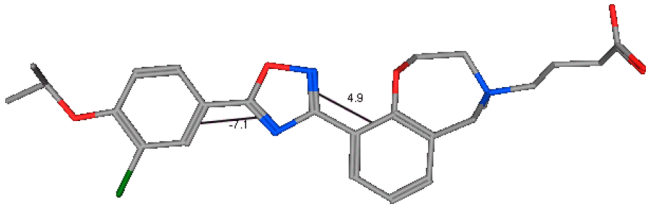

Figure 5. X-ray crystal structure of benzoxazepine **26a**.

a more lipophilic core template such as benzazepine would deliver improved pharmacokinetics for compounds possessing this more polar substituent. The N-linked benzazepinyl butanoic acid **27c** showed a pEC_{50} value of 8.0 against $S1P_1$ and ~1000-fold selectivity over $S1P_3$ receptors (Table 5). The CHI log *D* for **27c** was found to be 1.78 at pH 7.4, in between the value for poorly active **28b** and efficacious compounds such as **28a** and **26a** (Table 8). Promisingly, **27c** was found to have similar *in vitro* permeability to **26a** and was found to be stable in hepatocytes across all four tested species. Moreover, following 1 mg/kg iv and 3 mg/kg oral doses in rats, it was found to have low blood clearance and good bioavailability. A similar study in the dog also revealed low clearance and good bioavailability. In the lymphopenia assay the excellent pharmacokinetics and higher *in vitro* potency of **27c** delivered a superior profile to **26a**, with the 0.3, 1, and 3 mg/kg doses delivering a full, prolonged lymphopenia (Figure 6). PK/PD calculations indicated a higher *in vivo* potency for **27c** with an IC_{50} of 15 nM. However, solubility screening for **27c** revealed no significant improvement when compared with **26a**.

Another approach to improving the solubility of these compounds was to introduce a heteroatom into the terminal phenyl ring. Replacement of the terminal phenyl ring of **30b** with a pyridyl ring gave **31**, which lowered the CHI log *D* from 2.02 to 1.74. Although this led to a modest loss of potency in the $S1P_1$ GTPgS assay, potency was largely maintained in the β-arrestin assay developed toward the end of this program (Table 6). Selectivity for $S1P_1$ over $S1P_3$ remained >100-fold. Compound **31** is stable in the intrinsic clearance assay in the

dx.doi.org/10.1021/jm5010336 | J. Med. Chem. XXXX, XXX, XXX−XXX

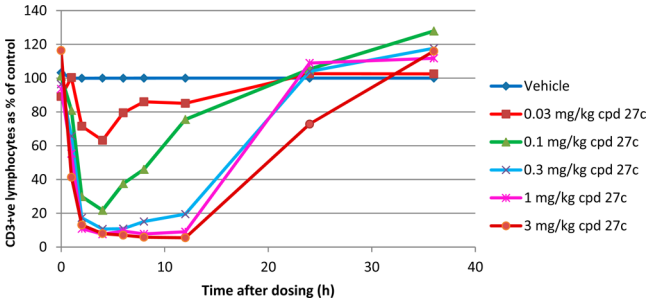

Figure 6. Effect of a range of doses of compound **27c** on CD3+ lymphocyte counts in rat blood.

presence of rat, mouse, cynomolgus monkey, and human hepatocytes, with some turnover in the dog; as with compound **26a**, plasma protein binding was high (Table 8). Compound **31** showed low clearance and a significantly reduced volume of distribution in the rat compared with **26a**, and good bioavailability was achieved following a 3 mg/kg oral dose. This compound was separated into enantiomers **31a** and **31b**, which showed similar potencies vs $S1P_1$ receptors and were both progressed to the rat lymphopenia assay. At a dose of 1 mg/kg both enantiomers delivered a >80% reduction in lymphocyte count from 2 to 12 h (Figure 7). Compound

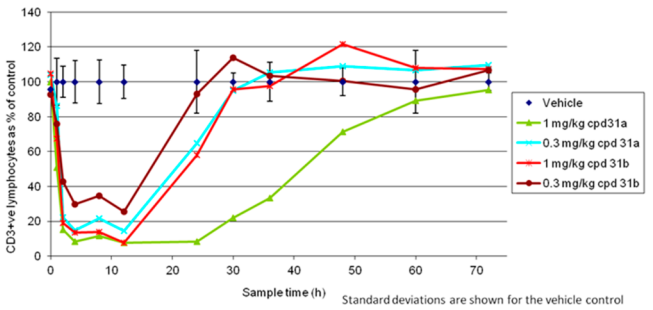

Figure 7. Effect of single oral doses of compounds **31a** and **31b** on CD3+ lymphocyte counts in rat blood.

31a exhibited a prolonged lympophenia, with effects on lymphocyte counts lasting at least 48 h,[41] whereas the lymphocyte counts for **31b** returned to baseline levels by 30 h. At 0.3 mg/kg, **31a** showed a similar profile to **31b** at the 1 mg/kg dose, whereas **31b** showed a slightly weaker effect with lymphocyte levels of 20−40%. *In vivo* IC_{50}'s for **31a,b** were 91 and 99 nM, respectively, reflecting somewhat lower *in vitro* potencies compared with **27c**.

Synthesis. The synthesis of compounds **8**−**31** is summarized in Schemes 1−14, with the exception of compounds **13** and **17b**, which have been described previously.[26] The pyrazole-containing compound **8** was prepared by converting the known alcohol **33**[17] to the corresponding benzylic bromide **34**, followed by displacement of the bromide with pyrazole-4-carboxylic acid ethyl ester and saponification to give the desired carboxylic acid derivative (Scheme 1). The 5-substituted indazole **9** was prepared starting from commercially available 5-cyanoindazole **35** (Scheme 2). First, the propanoic ester group was introduced by reaction with ethyl 3-bromopropanoate, and the cyano group was converted to the amidoxime **36** using hydroxylamine. Coupling to 3-chloro-4-isopropoxybenzoic acid using EDC and HOBt followed by heating effected cyclization to the oxadiazole, and finally saponification gave the desired acid **9**. The isomeric 4-substituted indazole **10** was prepared starting from 2-amino-6-bromotoluene **37** (Scheme 3). Conversion to 4-bromoindazole **38** was effected by diazotization of the aminotoluene with isoamyl nitrite and cyclization under basic conditions. Next, the 4-bromoindazole was substituted as above using ethyl 3-bromopropionate, and Pd-catalyzed reaction with zinc cyanide gave the 4-cyanoindazole intermediate **39**. This was converted to the amidoxime **40** as before, and reaction with 3-chloro-4-isopropoxybenzoyl chloride followed by heating in DMF gave the oxadiazole intermediate, which was saponified to give the desired compound **10**.

The synthesis of compounds **11a,b** and **21a**−**c** required preparation of the 4-substituted isoindoline template (Scheme 4). This was effected by double radical bromination of 2,3-dimethylbenzonitrile **41**, followed by cyclization with benzylamine to give **43**. Next, the benzyl group was removed using chloroethyl chloroformate, and the nitrogen was reprotected using Boc anhydride. Conversion of the nitrile to the amidoxime **44** as above followed by acylation with 3-chloro-4-isopropoxybenzoic acid and cyclization gave the oxadiazole, and finally deprotection with TFA gave the desired isoindoline **11a**. Compounds **21a**−**c** were synthesized by reaction of the

Scheme 1. Compound 8[a]

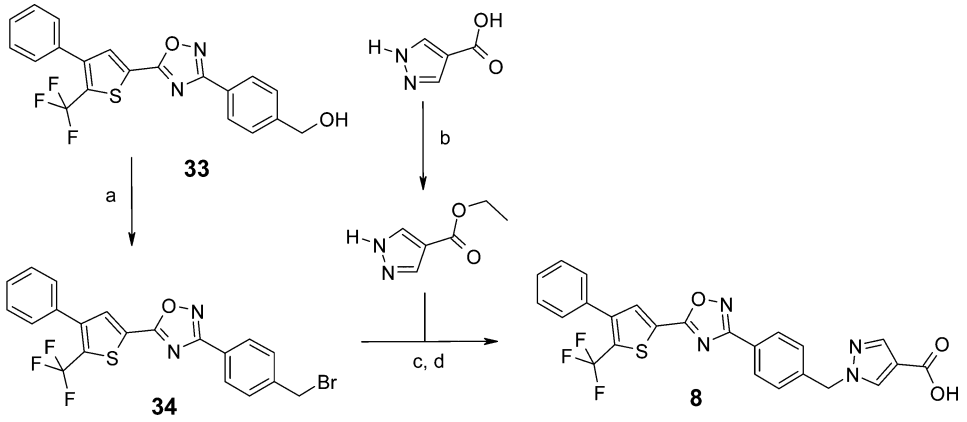

[a]Reagents and conditions: (a) PPh_3, NBS, THF, 0 °C; (b) H_2SO_4, EtOH, reflux, 97%; (c) KO^{t}Bu, EtOH, 60 °C, 63% (2 steps); (d) LiOH, H_2O, EtOH, 40 °C, 62%.

dx.doi.org/10.1021/jm5010336 | J. Med. Chem. XXXX, XXX, XXX−XXX

Scheme 2. Compound 9[a]

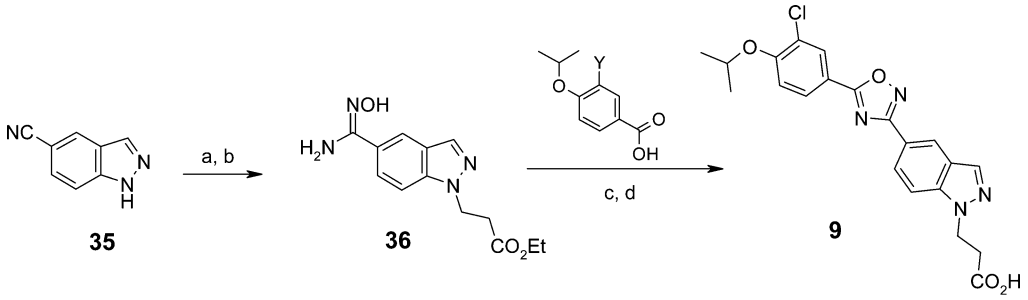

[a]Reagents and conditions: (a) $BrCH_2CH_2CO_2Et$, Cs_2CO_3, DMF, 80 °C, 66%; (b) $NH_2OH{\cdot}HCl$, $NaHCO_3$, EtOH, 50 °C, 87%; (c) EDC, HOBt, DMF, 120 °C, 58%; (d) NaOH, EtOH, room temperature, 55%.

Scheme 3. Compound 10[a]

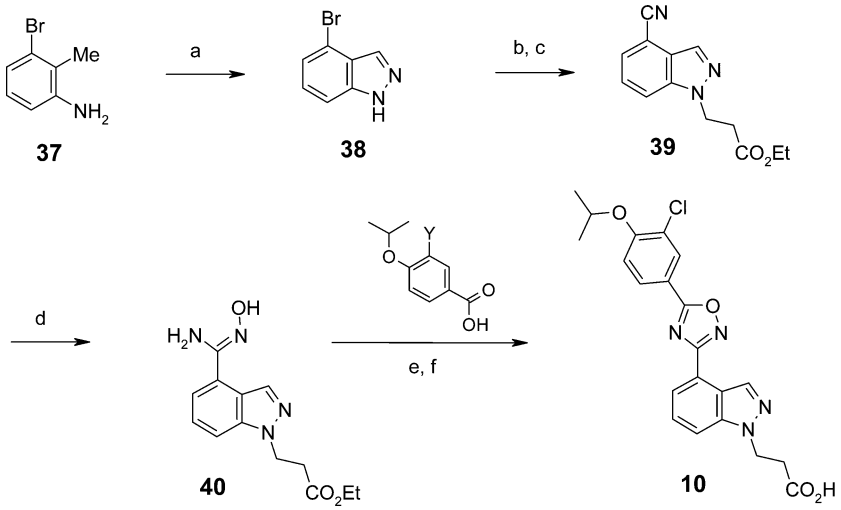

[a]Reagents and conditions: (a) (i) Ac_2O, AcOK, isoamyl nitrite, $CHCl_3$, 0−60 °C; (ii) conc. HCl then NaOH, 0−30 °C, 91%; (b) ethyl acrylate, DBU, CH_3CN, 70 °C, 78%; (c) $Zn(CN)_2$, $Pd(PPh_3)_4$, 1,4-dioxane, reflux, 78%; (d) $NH_2OH{\cdot}HCl$, $NaHCO_3$, EtOH, reflux, 80%; (e) (i) acid, $(COCl_2)_2$, DMF cat., CH_2Cl_2, room temperature; (ii) hydroxyimidate, DMF, room temperature to 120 °C, 78%; (f) NaOH, $EtOH/H_2O$, 60 °C, 99%.

corresponding isoindoline with either ethyl 3-bromopropionate or ethyl 4-bromobutyrate followed by saponification.

Benzazepines **12a,b** and **22a,b** were prepared starting from Boc-protected 6-hydroxybenzazepine **45** (Scheme 5).[42] Reaction with triflic anhydride gave the triflate ester, which allowed Pd-catalyzed introduction of the nitrile substituent with zinc cyanide to give **46**. Conversion to the amidoxime **47** as before followed by reaction with either 3-chloro- or 3-cyano-4-isopropoxybenzoic acid methyl ester in the presence of sodium hydride effected cyclization to the corresponding oxadiazoles, and deprotection with TFA gave the desired benzazepines **12a** or **12b**. Compounds **22a,b** were prepared by alkylation of **12a** with *t*-butyl 3-bromopropionate or *t*-butyl 4-bromobutyrate, followed by acidic deprotection.

The 5-substituted tetrahydroisoquinolines **14a,b** were prepared starting from commercially available 5-cyanotetrahydroisoquinoline **48** (Scheme 6). Boc protection and conversion to the amidoxime **49** followed by reaction with 3-chloro-4-isopropoxybenzoic acid methyl ester in the presence of sodium hydride effected cyclization to the corresponding oxadiazole, and deprotection with TFA gave the desired THIQ **14a**. N-alkylation of **14a** with ethyl bromoacetate followed by saponification gave the amino acid **25**. The C-linked amino acids **28a,b** were prepared by NBS-mediated oxidation of **14a** or **14b** to give the corresponding dihydroisoquinoline, followed by addition of mono *t*-butyl malonate and acidic ester hydrolysis or of monoethyl malonate and saponification, respectively.

The 6-substituted benzoxazepine **15a** was prepared from the previously described amidoxime **50**[26] (Scheme 7) by cyclization with 3-chloro-4-isopropoxybenzoyl chloride to give the oxadiazole followed by deprotection with hydrochloric acid. N-alkylation of **15a** with ethyl 4-bromobutyrate followed by saponification gave the N-linked acid **26**.

Synthesis of the isomeric benzoxazepines **16a,b** and **23a−c** required preparation of the corresponding template (Scheme 8). Starting with methyl 2-hydroxy-5-bromobenzoate **51**, Mitsunobu condensation with N-Boc ethanolamine **52** followed by acidic deprotection and cyclization under basic conditions gave the benzoxazepinone **54**. Next, reduction with borane·THF complex followed by Boc protection of the resulting benzoxazepine allowed Pd-catalyzed introduction of the nitrile group using zinc cyanide. Conversion to the amidoxime **55** as before followed by EDC/HOBt mediated coupling with 3-chloro- or 3-cyano-4-isopropoxybenzoic acid and heat effected cyclization to the oxadiazole, and deprotection with hydrochloric acid gave the desired benzoxazepines **16a** or **16b**. N-alkylation of **16a** with ethyl 3-bromopropionate

dx.doi.org/10.1021/jm5010336 | J. Med. Chem. XXXX, XXX, XXX−XXX

Scheme 4. Compounds 11a,b and 21a−c[a]

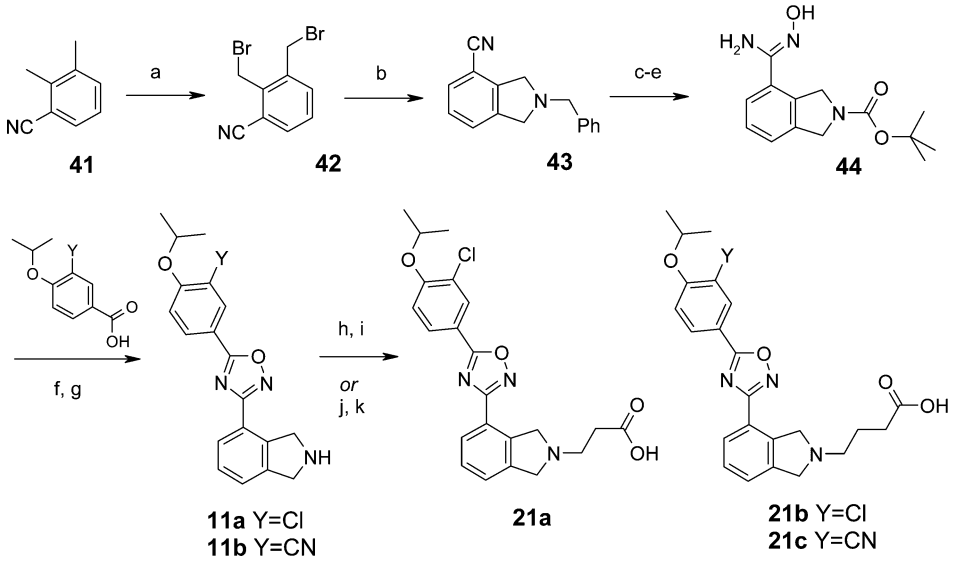

[a]Reagents and conditions: (a) NBS, $(PhCO_2)_2$, CCl_4, 80 °C; (b) $PhCH_2NH_2$, Na_2CO_3, MeCN, 80 °C, 25% (2 steps); (c) $ClCH_2CH_2OCOCl$, 4 Å sieves, PhCl, 90 °C, 79%; (d) Boc_2O, Et_3N, DCM, 34%; (e) $NH_2OH{\cdot}HCl$, $NaHCO_3$, EtOH, 50 °C, 58%; (f) EDC, HOBt, DMF, room temperature to 120 °C, 28% (**11a**), 11% (**11b**); (g) TFA, DCM, room temperature, 96% (**11a**), 88% (**11b**) ; (h) $Br(CH_2)_2CO_2Et$, $EtN(iPr)_2$, MeCN, 80 °C, 93% (**21a**); (i) NaOH, EtOH/water, room temperature, 41% (**21a**); (j) $Br(CH_2)_3CO_2Et$, $EtN(iPr)_2$, MeCN, 80 °C, 92% (**21b**), 83% (**21c**); (k) NaOH, EtOH/water, room temperature, 33% (**21b**), 16% (**21c**).

Scheme 5. Compounds 12a,b and 22a,b[a]

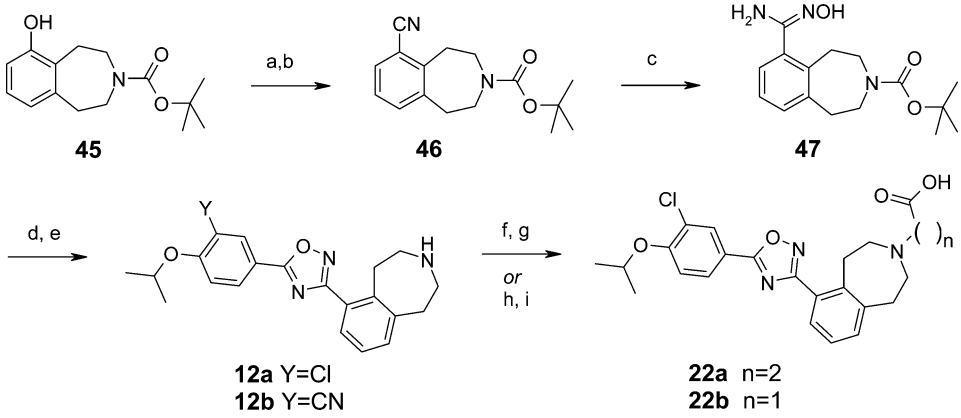

[a]Reagents and conditions: (a) Tf_2O, Et_3N, DCM, −10 °C, 51%; (b) $Zn(CN)_2$, $Pd(PPh_3)_4$, DMF, 150 °C, 99%; (c) $NH_2OH{\cdot}HCl$, $NaHCO_3$, EtOH, 50 °C, 39%; (d) NaH, 3-Cl-4-^{i}PrO-$PhCO_2Me$ or 3-CN-4-^{i}PrO-$PhCO_2Me$, THF, reflux, 96% (**12a**), 86% (**12b**); (e) TFA, DCM, reflux (100%, **12a,b**); (f) $Br(CH_2)_2CO_2tBu$, K_2CO_3, DMF, 100 °C, 25% (**22a**); (g) HCl, 1,4-dioxane, room temperature, 54% (**22a**); (h) $BrCH_2CO_2tBu$, K_2CO_3, DMF, 100 °C, 92% (**22b**); (i) HCl, 1,4-dioxane, room temperature, 94% (**22b**).

or of **16b** with ethyl 3-bromopropionate or ethyl 4-bromobutyrate followed by saponification gave the acids **23a−c**, respectively.

The 7-substituted benzazepine **17a** was prepared from the previously described 5-cyanobenzazepine **56**[26] (Scheme 9). Conversion to the amidoxime followed by coupling to 4-chloro-3-isopropoxybenzoic acid using EDC/HOBt and heating effected cyclization to the oxadiazole, and Boc deprotection using hydrochloric acid gave **17a**. N-alkylation of **17a** with *t*-butyl acrylate followed by acidic deprotection gave the acid **27b**. N-alkylation of **17b** with ethyl bromoacetate or ethyl 4-bromobutyrate followed by saponification gave the acids **27a** and **27c**, respectively.

The benzoxazepine isomers **18a** and **18b** were prepared starting from 4-methoxysalicylic acid methyl ester **57** (Scheme 10). Mitsunobu condensation with N-Boc ethanolamine followed by acidic deprotection and cyclization under basic conditions gave the benzoxazepinone **59**. Next, the methyl ether was hydrolyzed using HBr, the resulting hydroxy group was reprotected by reaction with benzyl bromide, and reduction of the lactam with lithium aluminum hydride then gave the benzoxazepine **60**. Boc N-protection, hydrogenolytic deprotection of the benzyl group, and conversion of the resulting hydroxy group to the triflate ester allowed Pd-catalyzed introduction of the nitrile group using zinc cyanide to give **61**. Conversion to the amidoxime as before followed by EDC/HOBt mediated coupling with 3-chloro- or 3-cyano-4-isopropoxybenzoic and heat effected cyclization to the oxadiazole, and deprotection with hydrochloric acid gave the desired benzoxazepines **18a** or **18b**.

dx.doi.org/10.1021/jm5010336 | J. Med. Chem. XXXX, XXX, XXX−XXX

Scheme 6. Compounds 14a,b, 25, and 28a,b[a]

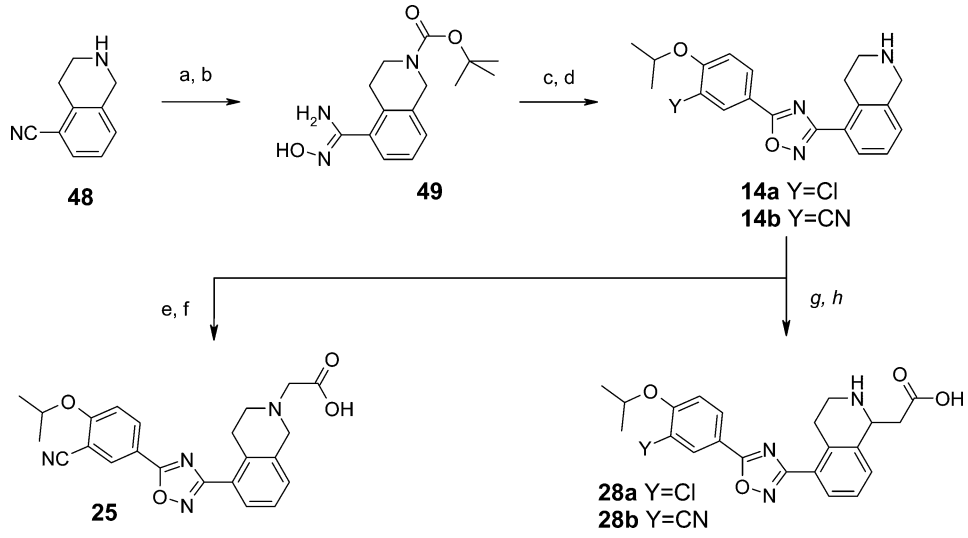

[a]Reagents and conditions: (a) Boc_2O, DCM, room temperature, 66%; (b) $NH_2OH{\cdot}HCl$, $NaHCO_3$, EtOH, 65 °C, 91%; (c) NaH, 3-Cl-4-^{i}PrO-$PhCO_2Me$, THF, reflux, 80% (**14a**) or 3-CN-4-^{i}PrO-PhCOCl, DIPEA, DMAP, DMF, 95 °C, 31% (**14b**); (d) HCl, 1,4-dioxane, room temperature, 90% (**14a**), 76% (**14b**); (e) $BrCH_2CO_2Et$, Cs_2CO_3, DMF, 60 °C, 32%; (f) LiOH, THF/MeOH/water, 100 °C, 85%; (g) NBS, DCM, microwave, 100 °C for (**28a**), or NBS, DCM, reflux for (**28b**), 45%; (h) **28a**, $tBuO_2CCH_2CO_2H$, K_2CO_3, MeCN, microwave 100 °C, 51% (2 steps) followed by HCl, 1,4-dioxane, room temperature, 92%; **28b**, $EtO_2CCH_2CO_2H$, K_2CO_3, THF, microwave 100 °C followed by LiOH, MeOH/THF/water, microwave 100 °C, 21% (2 steps).

Scheme 7. Compounds 15a and 26[a]

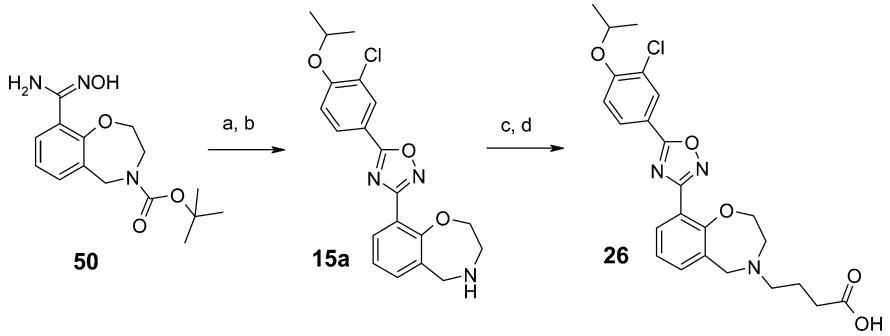

[a]Reagents and conditions: (a) (i) 3-Cl-4-^{i}PrO-$PhCO_2Cl$, $(COCl_2)_2$, DMF cat., DCM, room temperature; (ii) amidoxime, DMF, room temperature to 120 °C, 82% (2 steps); (b) HCl, 1,4-dioxane, room temperature, 99%; (c) $Br(CH_2)_3COOC_2H_5$, K_2CO_3, DMF, 80 °C, 70%; (d) NaOH, EtOH/H_2O, room temperature, 79%.

The 7-substituted benzazepines **19a** and **19b** were prepared according to Scheme 11. Starting with 7-amino-benzazepinone **62**, diazotization and reaction with triiodomethane followed by reduction of the lactam with $BH_3{\cdot}THF$ complex afforded the 7-iodobenzazepine **63**. Boc-protection of the nitrogen followed by Pd-catalyzed reaction with zinc cyanide gave the nitrile, which was converted as before to the amidoxime **64**. EDC/HOBt mediated coupling with 3-chloro- or 3-cyano-4-isopropoxybenzoic and heat effected cyclization to the oxadiazole, and deprotection with hydrochloric acid gave the desired benzazepines **19a** or **19b**.

The benzazepine isomer **20** was prepared starting from 2,6-dicyanotoluene **65** (Scheme 12). Reaction with hydroxylamine gave the monoamidoxime, which was acylated by 3-chloro-4-isopropoxybenzoic methyl ester in the presence of sodium hydride and heated to form the oxadiazole **66**. Next, the methyl group was deprotonated with LDA, and the resulting anion was treated with allyl bromide. The resulting alkene **67** was converted to the alcohol by ozonolysis followed by treatment with borane·DMS complex, which also effected reduction of the nitrile to the benzylic amine **68**. This amino alcohol was cyclized under Mitsunobu conditions to give the desired benzazepine **20**.

The C-linked benzoxazepine acids **29a,b** were prepared using a similar sequence to compounds **16a,b** (Scheme 13). Starting with methyl 2-hydroxy-5-bromobenzoate **51**, Mitsunobu condensation with protected propanediol **69** followed by acidic deprotection and cyclization under basic conditions gave the hydroxymethyl benzoxazepinone **71**. Next, reduction with borane·THF complex followed by Boc protection of the resulting benzoxazepine allowed Pd-catalyzed introduction of the nitrile group using zinc cyanide to give **72**. Conversion to the amidoxime as before followed by EDC/HOBt mediated coupling with 3-chloro-4-isopropoxybenzoic effected cyclization to the oxadiazole **73**. Oxidation of the hydroxymethyl group under Jones conditions and acidic deprotection gave the desired benzoxazepine **29a**. Alternatively, the hydroxymethyl group was oxidized to the aldehyde using Dess–Martin

dx.doi.org/10.1021/jm5010336 | J. Med. Chem. XXXX, XXX, XXX–XXX

Scheme 8. Compounds 16a,b and 23a−c[a]

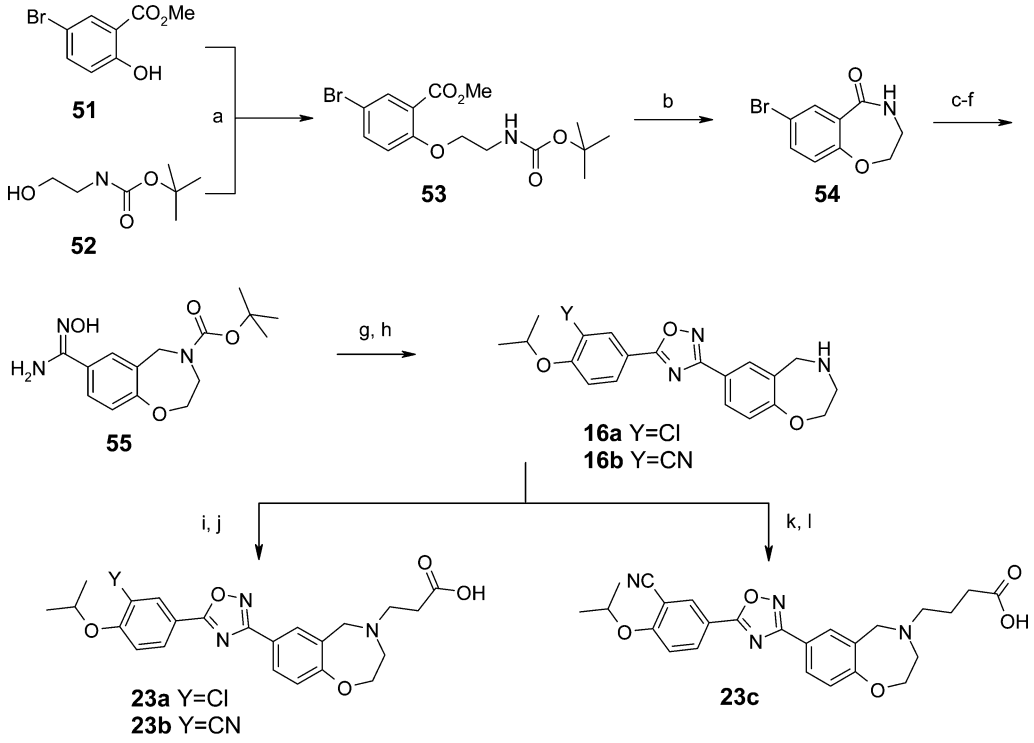

[a]Reagents and conditions: (a) DIAD, PPh_3, THF, room temperature, 55%; (b) TFA, DCM, room temperature; then Et_3N, toluene, 100 °C, 59%; (c) BH_3.THF, THF, room temperature to 65 °C, 97%; (d) Boc_2O, Et_3N, DCM, room temperature, 89%; (e) $Zn(CN)_2$, $Pd(PPh_3)_4$, DMF, 80 °C, 90%; (f) NH_2OH·HCl, $NaHCO_3$, EtOH, 60 °C, 78%; (g) 4-Cl-3-iPrOPhCO_2H or 4-CN-3-iPrOPhCO_2H, EDC, HOBt, DMF, room temperature to 120 °C, 31% (**16a,b**); (h) HCl, 1,4-dioxane, room temperature, 71% (**16a**), 73% (**16b**); (i) $Br(CH_2)_2CO_2Et$, $EtN(iPr)_2$, MeCN, 80 °C, 97% (**23a**), 72% (**23b**); (j) NaOH, EtOH/water, room temperature, 47% (**23a**), 10% (**23b**); (k) $Br(CH_2)_3CO_2Et$, $EtN(iPr)_2$, MeCN, 80 °C, 62%; (l) NaOH, EtOH/water, room temperature, 28%.

Scheme 9. Compounds 17a,b and 27a−c[a]

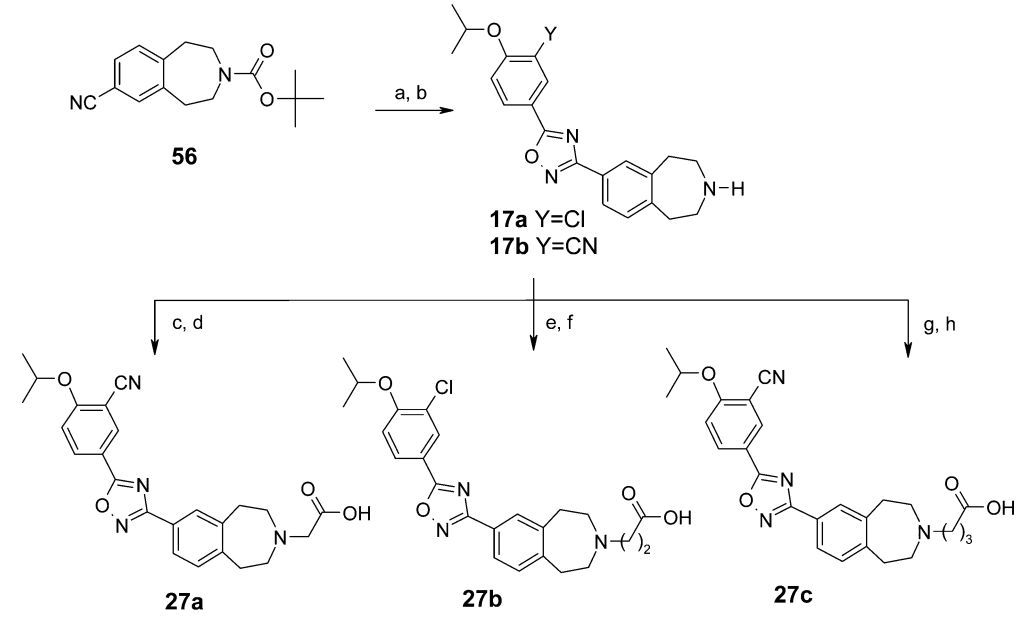

[a]Reagents and conditions: (a) NH_2OH·HCl, $NaHCO_3$, EtOH, 60 °C, 93%; (b) 4-Cl-3-iPrOPhCO_2H, EDC, HOBt, DMF, room temperature to 120 °C, 29% (**17a**) or (i) 4-CN-3-iPrOPhCO_2H, $(COCl_2)_2$, DMF cat., CH_2Cl_2, room temperature; (ii) hydroxyimidate, toluene/pyridine, room temperature to reflux, 78%, (**17b**); (b) HCl, 1,4-dioxane, room temperature, 82% (**17a**), 95% (**17b**); (c) $BrCH_2CO_2Et$, Cs_2CO_3, DMF, room temperature to 60 °C, 62%; (d) NaOH, EtOH/H_2O, 40 °C, 89%; (e) *t*-butyl acrylate, $EtN(iPr)_2$, MeOH, 90 °C; (f) HCl, 1,4-dioxane, room temperature, 46% (2 steps); (g) $Br(CH_2)_3COOC_2H_5$, K_2CO_3, DMF, 90 °C, 90%; (h) NaOH, EtOH/H_2O, room temperature, 63%.

dx.doi.org/10.1021/jm5010336 | J. Med. Chem. XXXX, XXX, XXX−XXX

Scheme 10. Compounds 18a,b[a]

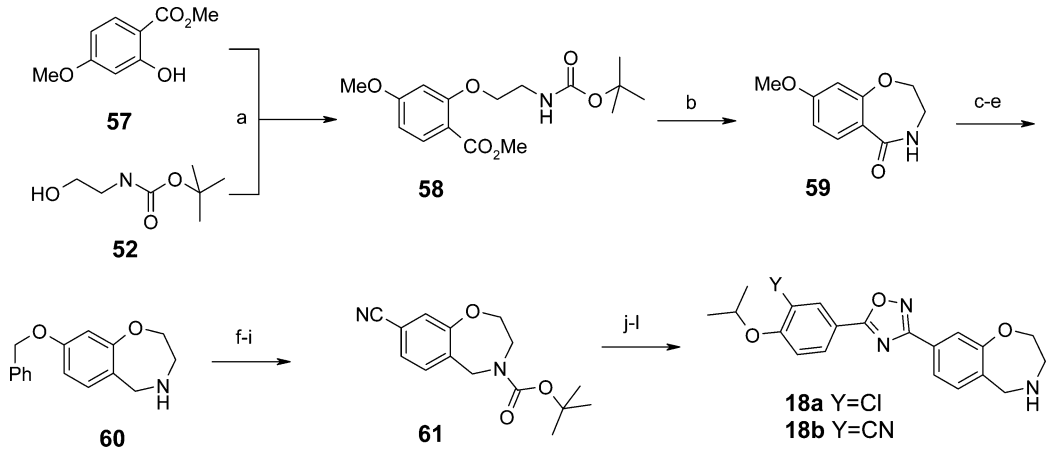

[a]Reagents and conditions: (a) DIAD, PPh_3, THF, 0 °C to room temperature; (b) TFA, DCM; then Et_3N, toluene, 100 °C, 44% (2 steps); (c) HBr, 110 °C; (d) BnBr, K_2CO_3, DMF, 60 °C, 75% (2 steps); (e) $LiAlH_4$, THF, 0−60 °C, 95%; (f) Boc_2O, Et_3N, DCM, room temperature, 70%; (g) H_2/Pd/C, THF/EtOH, room temperature, 100%; (h) Tf_2O, Py, 0 °C, 100%; (i) $Zn(CN)_2$, $Pd(PPh_3)_4$, DMF, 80 °C, 72%; (j) NH_2OH·HCl, $NaHCO_3$, EtOH, 60 °C, 96%; (k) 4-Cl-3-iPrOPhCO_2H or 4-CN-3-iPrOPhCO_2H, EDC, HOBt, DMF, room temperature to 120 °C, 56% (**18a**), 92% (**18b**); (l) HCl, 1,4-dioxane, room temperature, 76% (**18a**), 90% (**18b**).

Scheme 11. Compounds 19a,b[a]

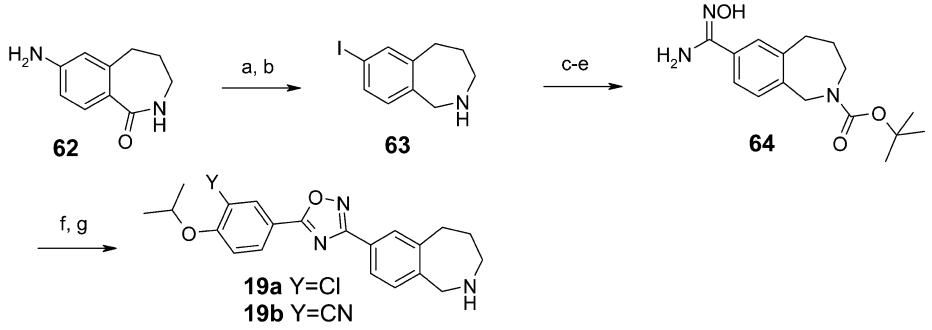

[a]Reagents and conditions: (a) CHI_3, tBuONO, THF, room temperature to 50 °C, 68%; (b) BH_3·THF, THF, reflux, 76%; (c) Boc_2O, Et_3N, DCM, room temperature, 100%; (d) $Zn(CN)_2$, $Pd(PPh_3)_4$, DMF, 80 °C, 74%; (e) NH_2OH·HCl, $NaHCO_3$, EtOH, 55 °C, 82%; (f) 4-Cl-3-iPrOPhCO_2H or 4-CN-3-iPrOPhCO_2H, EDC, HOBt, DMF, room temperature to 90 °C, 16% (**19a**), 46% (**19b**); (g) HCl, 1,4-dioxane, room temperature, 69% (**19a**), 86% (**19b**).

Scheme 12. Compound 20[a]

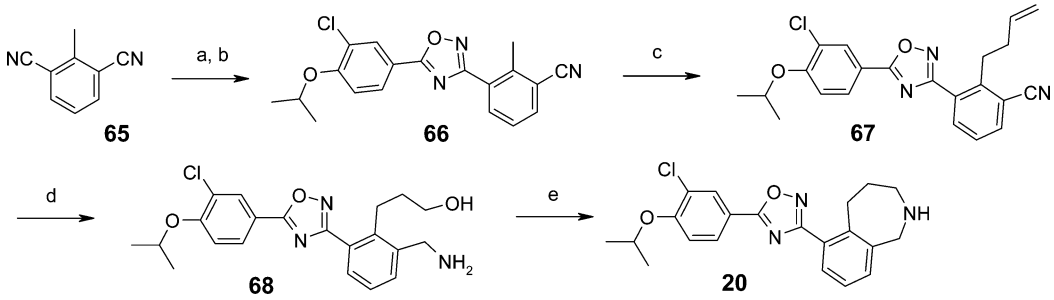

[a]Reagents and conditions: (a) NH_2OH·HCl, $NaHCO_3$, EtOH, 60 °C, 51%; (b) NaH, 4-Cl-3-iPrOPhCO_2Me, THF, room temperature to reflux, 90%; (c) LDA, THF, AllBr, −78 °C, 60%; (d) O_3, DCM, −78 °C; then THF, BH_3·DMS, room temperature to 40 °C, 19%; (e) DIAD, PPh_3, DCM, room temperature, 13%.

periodinane, allowing Wittig chain extension, hydrogenation, and saponification to give the C-linked propionic acid **29b**.

The C-linked benzoxazepine acids **30a,b** and **31a,b** again required de novo synthesis of the template (Scheme 14). Starting from 6-bromosalicylaldehyde **74**, Wittig condensation followed by Mitsunobu reaction gave the cinnamate ester **75**, and acidic Boc deprotection followed by heating under basic conditions effected a 7-exo cyclization to generate the benzoxazepine ring, which was then reprotected to give **76**. Next, the bromo substituent was replaced by cyano using palladium catalysis, and the ester group was converted to the alcohol **77** by lithium borohydride reduction. Pyridine sulfur

dx.doi.org/10.1021/jm5010336 | J. Med. Chem. XXXX, XXX, XXX−XXX

Scheme 13. Compounds 29a,b[a]

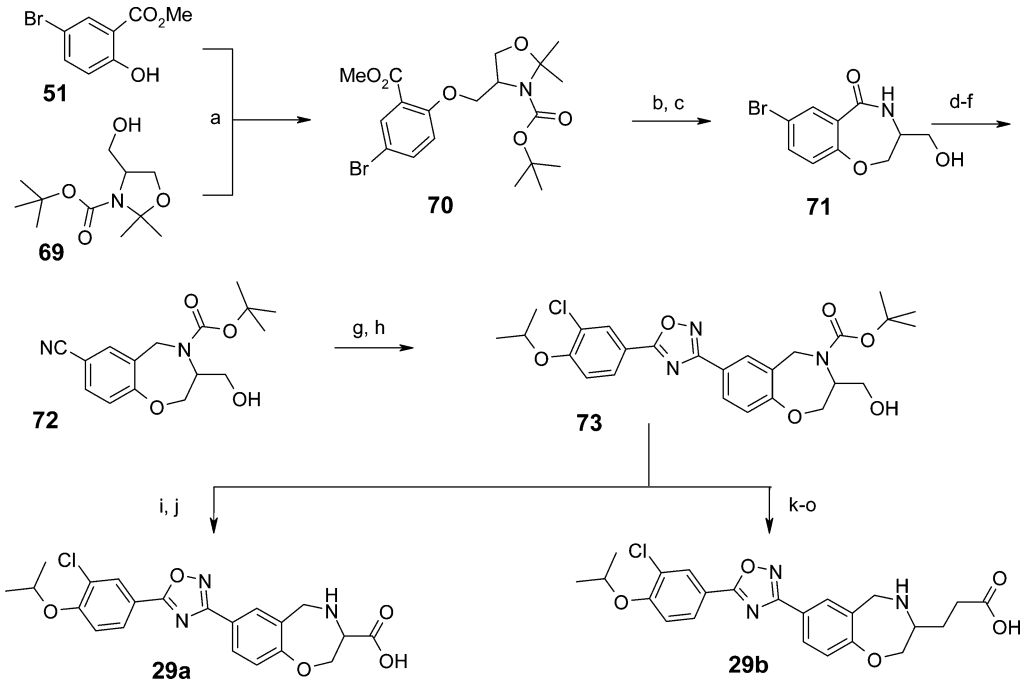

[a]Reagents and conditions: (a) DIAD, PPh_3, toluene, 80 °C, 57%; (b) p-TsOH, MeOH, room temperature, 81%; (c) TFA, DCM, room temperature; then Et_3N, toluene, 100 °C, 73%; (d) BH_3·THF, THF, room temperature to 65 °C, 86%; (e) Boc_2O, aqueous Na_2CO_3, THF, room temperature, 88%; (f) $Zn(CN)_2$, $Pd(PPh_3)_4$, DMF, 80 °C, 82%; (g) NH_2OH·HCl, $NaHCO_3$, EtOH, 50 °C, 95%; (h) 4-Cl-3-iPrOPhCO$_2$H, EDC, HOBt, DMF, room temperature to 100 °C, 28%; (i) CrO_3, H_2SO_4, acetone, 0 °C, 68%; (j) HCl, 1,4-dioxane, room temperature, 64%; (k) Dess–Martin, DCM, room temperature, 88%; (l) Ph_3PCHCO_2Et, THF, 40 °C, 71%; (m) H_2/Pd/C, EtOH, room temperature, 54%; (n) aq NaOH, EtOH, room temperature, 98%; (o) HCl, 1,4-dioxane, room temperature, 61%.

trioxide oxidation to the corresponding aldehyde followed by Wittig homologation and PCC oxidation gave the C-propionyl ester **78**, which was converted to **30a** by the usual sequence of amidoxime formation, cyclization, and deprotection. Alternatively, Wittig reaction of the aldehyde gave the unsaturated ester **79**, which was reduced by hydrogenolysis to the C-butyryl ester and converted to **30b** or **31a,b** using the usual sequence of amidoxime, cyclization, and deprotection. Compound **30b** was isolated as the racemate, while the enantiomers **31a** and **31b** were separated by chiral chromatography prior to deprotection.

CONCLUSIONS

In this study, we have identified a range of novel $S1P_1$ receptor agonists with promising developability properties. Starting with a carboxylic acid-based template, we found that reducing lipophilicity and enhancing potency by using the bicyclic indazole template allowed maximal sustained lymphopenia in rats to be achieved at 1 mg/kg. Replacement of the fused aromatic bicyclic template with basic aromatic-saturated fused bicycles also afforded compounds showing maximal lymphopenia at 1 mg/kg, despite their significant differences in volumes of distribution compared with the acidic analogues. Design of related bicyclic zwitterionic compounds allowed further enhancement of properties, such that similar lymphopenia could be achieved at the lower dose of 0.3 mg/kg with either the N-linked benzoxazepine **26a** or the C-linked benzoxazepines **31a,b**. The N-linked benzazepine **27c** even demonstrated efficacy at doses as low at 0.1 mg/kg po. This progress was aided by systematically exploring the effects of molecular properties on permeability, free fraction, and solubility. Establishing a correlation between *in vitro* and *in vivo* potency[32] accelerated compound selection and enabled the prioritization of compounds for *in vivo* studies. Definitive PK/PD relationships were established using the rat lymphopenia model, which also facilitated an early estimation of human dose.[32] Overall, solubility for the different chemotypes discussed here remained low, despite efforts to introduce charged groups and break the planarity of the compounds to reduce crystal lattice energy. However, despite this shortcoming, good bioavailability was achieved, most likely due to good permeability, which compensated for the low solubility. This campaign resulted in the identification of several potent $S1P_1$ receptor agonists with appropriate developability properties suitable for further progression to preclinical development.

EXPERIMENTAL SECTION

General. All solvents were purchased from Romil Ltd. (Hy-Dry anhydrous solvents), and commercially available reagents were used as received. Melting points were recorded on a Buchi B-545 apparatus and are uncorrected. All reactions were followed by TLC analysis (TLC plates GF254, Merck) or LCMS (liquid chromatography mass spectrometry) using a Waters ZQ instrument. NMR spectra were recorded on a Bruker AVANCE 400 spectrometer and are referenced as follows: ^1H (400 MHz), internal standard TMS at δ = 0.00; ^{13}C (100.6 MHz), internal standard $CDCl_3$ at δ = 77.23 or DMSO-d_6 at δ = 39.70. Column chromatography was performed on prepacked silica gel columns (3090 mesh, IST) using a biotage SP4. Mass spectra were recorded on Waters ZQ (ESI-MS) and Q-Tof 2 (HRMS) spectrometers. Mass directed auto prep was performed on a Waters 2767 instrument with a MicroMass ZQ mass spectrometer using a Supelco LCABZ++ column. GLOBAL gradients for chromatography are as follows (solvent B, polar component; CV = column volume): 10% GLOBAL, 3% B for 2 CV, 3–13% B over 10 CV, then 13% B for 5 CV; 20% GLOBAL, 5% B for 2 CV, 5–20% B over 10 CV, then 20%

dx.doi.org/10.1021/jm5010336 | J. Med. Chem. XXXX, XXX, XXX–XXX

Scheme 14. Compounds 30a,b and 31a,b[a]

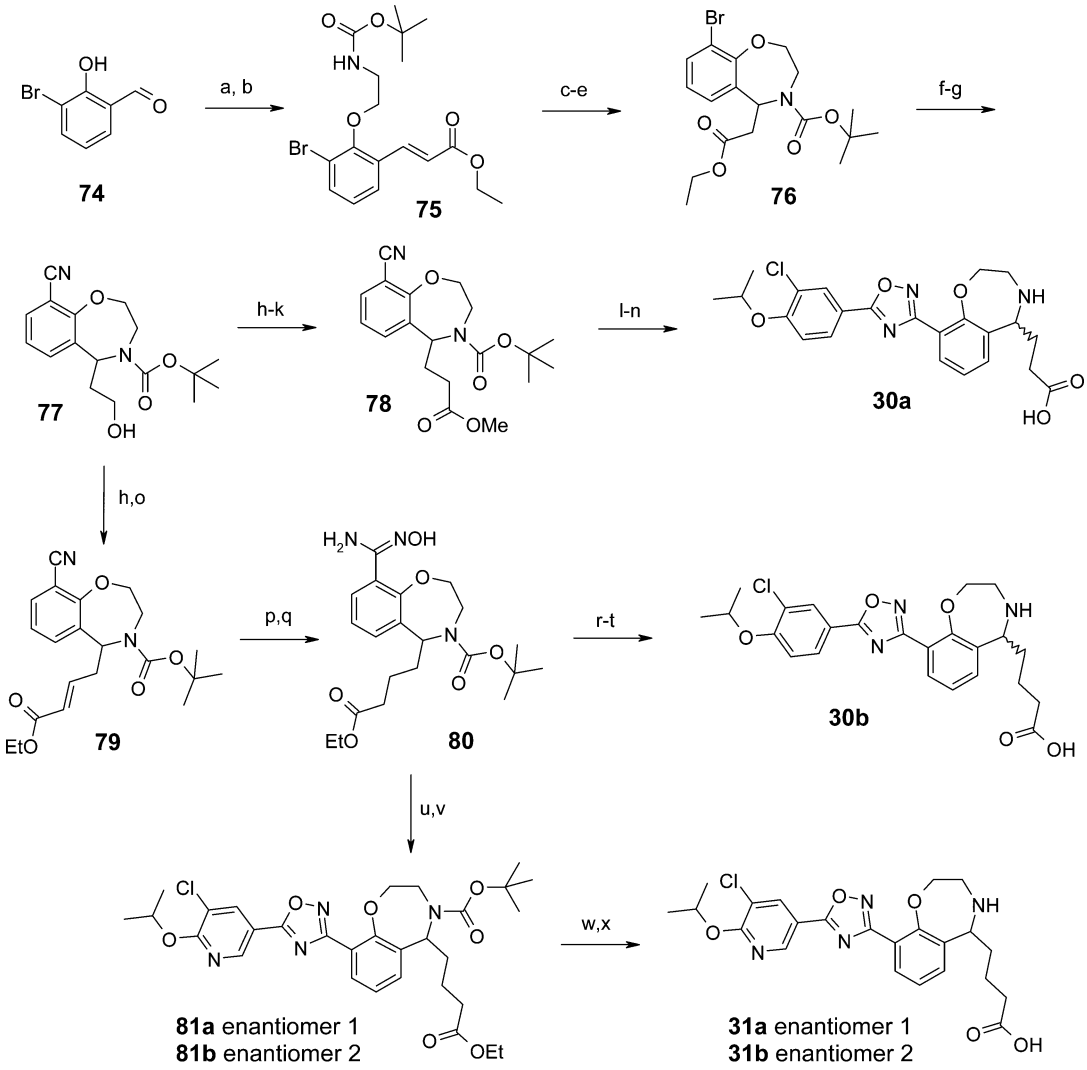

[a]Reagents and conditions: (a) $Ph_3P{=}CHCOOC_2H_5$, CH_2Cl_2, 0 °C, 95%; (b) $BocNH(CH_2)_2OH$, PPh_3, DIAD, THF, 0 °C, 94%; (c), CF_3COOH, CH_2Cl_2, room temperature, 100%; (d) DBU, THF, 60 °C, 97%; (e) Boc_2O, NEt_3, CH_2Cl_2, room temperature, 92%; (f) $Zn(CN)_2$, $Pd(PPh_3)_4$, DMF, 96 °C, 92%; (g) $LiBH_4$, EtOH/Et_2O, room temperature, 96%; (h) DMSO, DIPEA, then $Py.SO_3$, Py, 0 °C, 100%; (i) Ph_2POCH_2OMe, LDA, THF, −78 °C to room temperature, then NaH, THF, room temperature, 42% (2 steps); (j) PCC, DCM, room temperature, 56% ; (k) $NH_2OH{\cdot}HCl$, $NaHCO_3$, MeOH, reflux, 100%; (l) 4-Cl-3-iPrOPhCO$_2$Cl, Et_3N, MeCN, room temperature to 100 °C, 10%; (m) aqueous NaOH, EtOH, 60 °C, 85%; (n) HCl, 1,4-dioxane, room temperature, 35%; (o) $Ph_3P{=}CHCOOC_2H_5$, 0 °C to room temperature, 94%; (p) $NH_2CH_2CH_2NH_2$, Pd/C, H_2 (1 atm), EtOH, room temperature, 100%; (q) aqueous NH_2OH, EtOH, reflux, 96%; (r) 4-Cl-3-iPrOPhCO$_2$Cl, Et_3N, MeCN, room temperature to 100 °C, 12%; (s) aqueous NaOH, EtOH, 50 °C, 94%; (t) HCl, 1,4-dioxane, room temperature, 17%; (u) (i) acid, $(COCl_2)_2$, CH_2Cl_2, room temperature; (ii) hydroxyimidate, NEt_3, DMF, room temperature to 120 °C, 60%; (v) Separation of enantiomers by chiral chromatography, 95%; (w) NaOH, EtOH/H_2O, 50 °C, 93%; (x) HCl, 1,4-dioxane, room temperature, 76%.

B for 5 CV; 30% GLOBAL, 8% B for 2 CV, 8−38% B over 10 CV, then 38% B for 5 CV; 40% GLOBAL, 10% B for 2 CV, 10−50% B over 10 CV, then 50% B for 5 CV; 50% GLOBAL, 13% B for 2 CV, 13−63% B over 10 CV, then 63% B for 5 CV; 100% GLOBAL, 25% B for 2 CV, 25−100% B over 10 CV, then 100% B for 10 CV. Abbreviations for multiplicities observed in NMR spectra are as follows: s, singlet; br s, broad singlet; d, doublet; t, triplet; q, quadruplet; p, pentuplet; spt, septuplet; m, multiplet. All compounds reported are of at least 95% purity according to LCMS (conditions described in the Supporting Information).

(*E*)-Ethyl 3-(3-Bromo-2-(2-((tert-butoxycarbonyl)amino)-ethoxy)phenyl) Acrylate (75). A solution of 3-bromo-2-hydroxybenzaldehyde **74** (10.05 g, 50 mmol) in CH_2Cl_2 (250 mL) at 0 °C under nitrogen was treated with ethyl (triphenyl-15-phosphanylidene)-acetate (17.4 g, 50 mmol), and the resulting mixture was stirred at this temperature for 30 min and then was concentrated *in vacuo*. Purification of the residue by flash chromatography on silica gel (5−25% EtOAc in hexanes) gave ethyl (2*E*)-3-(3-bromo-2-hydroxyphenyl)-2-propenoate (12.85 g, 95%) as a white solid. LCMS (method formate): retention time 0.82 min, $[M + H]^+$ = 273, 275 (1 Br). ^1H NMR (400 MHz, $CDCl_3$) δ ppm 7.93 (d, J = 16.2 Hz, 1H), 7.48 (dd, J = 8.1, 1.5 Hz, 1H), 7.44 (dd, J = 7.8, 1.3 Hz, 1H), 6.84 (t, J = 8.0 Hz, 1H), 6.58 (d, J = 16.2 Hz, 1H), 6.01 (s, 1H), 4.27 (q, J = 7.2 Hz, 2H), 1.34 (t, J = 7.2 Hz, 3H). A solution of this material (4.07 g, 15.0 mmol) and triphenylphosphine (4.33 g, 16.50 mmol) under nitrogen in THF (100 mL) at room temperature was treated with 1,1-dimethylethyl (2-hydroxyethyl)carbamate (2.32 mL, 15.0 mmol). The resulting yellow solution was cooled to 0 °C, and then DIAD (3.21 mL, 16.50 mmol) was added dropwise over 5 min. After 10 min, the ice bath was removed, and the mixture was stirred at room temperature for 1.5 h and then was concentrated *in vacuo*. The residue was dissolved in EtOAc, and the organic phase was washed

dx.doi.org/10.1021/jm5010336 | J. Med. Chem. XXXX, XXX, XXX−XXX

three times with brine, dried over $MgSO_4$, and concentrated *in vacuo*. Purification of the residue by flash chromatography on silica gel (5−25% EtOAc in hexanes) gave **33** (5.87 g, 14.17 mmol, 94% yield) as a white solid. LCMS (method formate): retention time 1.01 min, $[M + H]^+$ = 414, 416 (1 Br). ^1H NMR (400 MHz, $CDCl_3$) δ ppm 7.91 (d, J = 16.2 Hz, 1H), 7.45−7.65 (m, 2H) 7.03 (t, J = 8.0 Hz, 1H), 6.46 (d, J = 16.2 Hz, 1H), 5.15−5.37 (m, 1H), 4.28 (q, J = 7.1 Hz, 2H), 4.01 (t, J = 4.8 Hz, 2H), 3.57 (d, J = 5.1 Hz, 2H), 1.47 (s, 9H), 1.35 (t, J = 7.1 Hz, 3H).

***tert*-Butyl 9-Bromo-5-(2-ethoxy-2-oxoethyl)-2,3-dihydrobenzo[*f*][1,4]oxazepine-4(5*H*)-carboxylate (76).** A solution of ethyl (2*E*)-3-(3-bromo-2-{[2-({[(1,1-dimethylethyl)oxy]-carbonyl}amino)ethyl]oxy}phenyl)-2-propenoate, **75** (58.1 g, 140 mmol), in CH_2Cl_2 (150 mL) at room temperature was treated with CF_3COOH (108 mL, 1.4 mol), and the resulting mixture was stirred for 14 h at this temperature and then was concentrated *in vacuo*. The residue was suspended in water (300 mL), and the mixture was basified with a 2 N NaOH aqueous solution to pH 10. The aqueous phase was then extracted with EtOAc (2 × 200 mL). The combined organic phases were dried over $MgSO_4$ and concentrated *in vacuo* to give (*E*)-ethyl 3-(2-(2-aminoethoxy)-3-bromophenyl)acrylate (48.2 g, 153 mmol, 109% yield) as a white solid, which was carried through as is to the next step without purification. LCMS (method formate): retention time 0.61 min, $[M + H]^+$ = 314, 316 (1 Br). ^1H NMR (400 MHz, $CDCl_3$) δ ppm 7.96 (d, J = 16.2 Hz, 1H), 7.59 (dd, J = 8.0, 1.4 Hz, 1H), 7.51 (dd, J = 7.8, 1.3 Hz, 1H), 7.05 (t, J = 8.0 Hz, 1H), 6.46 (d, J = 16.2 Hz, 1H), 6.28 (br s, 2H), 4.25 (q, J = 7.1 Hz, 2H), 4.10−4.19 (m, 2H), 3.40 (t, J = 4.9 Hz, 2H), 1.29−1.33 (t, J = 7.1 Hz, 3H). A solution of this material (48.4 g, 137 mmol) in THF (200 mL) at room temperature was treated with DBU (25 mL, 166 mmol), and the resulting mixture was stirred at 60 °C for 16 h and then cooled to room temperature and concentrated *in vacuo*. The residue was dissolved in EtOAc (300 mL), and the organic phase was washed with water (2 × 300 mL) and then brine (100 mL), dried over $MgSO_4$, and concentrated *in vacuo* to give ethyl (9-bromo-2,3,4,5-tetrahydro-1,4-benzoxazepin-5-yl)acetate (41.9 g, 97%) as a pale yellow oil, which was used in the next step without further purification. LCMS (method formate): retention time 0.59 min, $[M + H]^+$ = 314, 316 (1 Br). ^1H NMR (400 MHz, $CDCl_3$) δ ppm 7.46 (dd, J = 8.1, 1.5 Hz, 1H), 7.10 (dd, J = 7.6, 1.3 Hz, 1H), 6.81−6.97 (m, 1H), 4.50 (dd, J,=,9.3, 5.8 Hz, 1H), 4.08−4.25 (m, 3H), 4.00 (ddd, J = 12.3, 7.5, 2.5 Hz, 1H), 3.44 (ddd, J = 14.7, 7.5, 2.5 Hz, 1H), 3.16 (ddd, J = 14.8, 5.8, 2.4 Hz, 1H), 3.07 (dd, J = 15.7, 9.3 Hz, 1H), 2.80 (dd, J = 15.5, 5.7 Hz, 1H), 1.75 (br s, 1H), 1.15−1.34 (m, 3H). A solution of this material (41.9 g, 133 mmol) and Et_3N (22.31 mL, 160 mmol) in CH_2Cl_2 (600 mL) was treated at room temperature with di-*tert*-butyl dicarbonate (34.1 mL, 147 mmol), and the resulting mixture was stirred for 18 h at room temperature. The organic phase was successively washed with water (400 mL), a 0.5 N HCl aqueous solution (300 mL), and brine (300 mL), dried over $MgSO_4$, and concentrated *in vacuo*. Purification of the residue by flash chromatography on silica gel (0−30% EtOAc in hexanes) gave **76** (50.7 g, 92%) as a white solid. LCMS (method formate): retention time 1.32 min, $[M + H]^+$ = 414, 416 (1 Br). ^1H NMR (400 MHz, DMSO-d_6) δ ppm 7.52 (dd, J = 8.0, 1.6 Hz, 1H), 7.22 (dd, J = 7.6, 1.5 Hz, 1H), 6.99 (t, J = 7.7 Hz, 1H), 5.52 (s, 1H), 4.36 (d, J = 9.9 Hz, 1H), 4.07 (q, J = 7.1 Hz, 2H), 3.98−4.04 (m, 1H), 3.73 (s, 1H), 3.63−3.68 (m, 1H), 3.10 (d, J = 8.1 Hz, 1H), 2.91−2.98 (m, 1H), 1.40 (s, 9H), 1.15−1.19 (m, 3H).

***tert*-Butyl 9-Cyano-5-(2-hydroxyethyl)-2,3-dihydrobenzo[*f*]-[1,4]oxazepine-4(5*H*)-carboxylate (77).** 1,1-Dimethylethyl 9-bromo-5-[2-(ethyloxy)-2-oxoethyl]-2,3-dihydro-1,4-benzoxazepine-4(5*H*)-carboxylate, **76** (70 g, 169 mmol), and $Zn(CN)_2$ (23.80 g, 203 mmol) were suspended in DMF (400 mL), and the resulting mixture was placed under vacuum for 5 min, then the flask was flushed with nitrogen. $Pd(PPh_3)_4$ (19.52 g, 16.90 mmol) was added, and the resulting mixture was stirred at 96 °C for 16 h under nitrogen and then was cooled to room temperature. The mixture was diluted with EtOAc (1 L) and filtered through Celite. The filtrate was washed with water (2 × 1 L) and brine (500 mL), dried over $MgSO_4$, and concentrated *in vacuo* to give a yellow oil. Purification of the residue by flash chromatography on silica gel (0−80% EtOAc in hexanes) gave *tert*-butyl 9-cyano-5-(2-ethoxy-2-oxoethyl)-2,3-dihydrobenzo[*f*][1,4]-oxazepine-4(5*H*)-carboxylate (56.1 g, 92%) as pale yellow solid. LCMS (method formate): retention time 1.32 min, $[M + H]^+$ = 361. ^1H NMR (250 MHz, DMSO-d_6) δ ppm 7.60−7.66 (m, 1H), 7.52−7.57 (m, 1H), 7.18−7.27 (m, 1H), 5.65 (s, 1H), 5.53−5.63 (m, 1H), 4.42−4.54 (m, 1H), 4.10 (m, 2H), 3.85−3.99 (m, 1H), 3.61−3.75 (m, 1H), 2.93−3.16 (m, 2H), 1.40 (s, 9H), 1.18 (t, J = 7.1 Hz, 3H). This material (59 g, 164 mmol) was dissolved in EtOH (200 mL) by heating to 60 °C, and the cooled solution (room temperature) was then diluted with Et_2O (900 mL). Lithium borohydride (2 M in THF, 246 mL, 491 mmol) was added under nitrogen, and the solution was stirred for 2 h at room temperature, giving a thick suspension. The mixture was treated slowly with MeOH (20 mL) and then added very cautiously to vigorously stirred water (300 mL). The mixture was extracted with EtOAc (200 mL). The organic phase was dried over $MgSO_4$ and concentrated *in vacuo* to give **77** (50.2 g, 96%), which was used in the next step without further purification. LCMS (method formate): retention time 0.92 min, $[M + H]^+$ = 318. ^1H NMR (400 MHz, $CDCl_3$) δ ppm 7.36−7.61 (m, 2H), 7.13 (t, J = 7.7 Hz, 1H), 5.55 (d, J = 5.6 Hz, 1H), 4.53 (dd, J = 12.6, 2.3 Hz, 2H), 4.08−4.36 (m, 1H), 3.81−4.01 (m, 1H), 3.45−3.70 (m, 3H), 2.27 (m, 1H), 1.96−2.16 (m, 1H), 1.46 (br s, 9H).

***(E)*-*tert*-Butyl 9-Cyano-5-(4-ethoxy-4-oxobut-2-en-1-yl)-2,3-dihydrobenzo[*f*][1,4]oxazepine-4(5*H*)-carboxylate (79).** A solution of 1,1-dimethylethyl 9-cyano-5-(2-hydroxyethyl)-2,3-dihydro-1,4-benzoxazepine-4(5*H*)-carboxylate, **77** (36 g, 102 mmol), in CH_2Cl_2 (300 mL) at 0 °C was treated with DMSO (35 mL) and DIPEA (62.2 mL, 356 mmol). In a separate flask, pyridine sulfur trioxide (32.4 g, 204 mmol) and pyridine (16.46 mL, 204 mmol) were mixed in DMSO (35 mL) for 10 min, and the mixture was added to the mixture of alcohol, base, and DMSO at 0 °C. The resulting mixture was stirred for 2 h at this temperature, until the alcohol was fully converted to the corresponding aldehyde. Ethyl 2-(triphenylphosphoranylidene)acetate (46.1 g, 132 mmol) was then added, and the resulting mixture was stirred at room temperature for 18 h. The mixture was diluted with CH_2Cl_2 (500 mL), washed successively with water (1 L), 10% citric acid in water (1 L), and water (1 L), and then dried over $MgSO_4$ and concentrated *in vacuo* to a pale yellow gum. Purification of the residue by flash chromatography on silica gel (0−30% EtOAc in hexanes) gave **79** (37.1 g, 94%) as pale yellow solid. LCMS (method formate): retention time 1.20 min, $[M + H]^+$ = 387. ^1H NMR (400 MHz, $CDCl_3$) δ ppm 7.31−7.63 (m, 2H), 7.13 (t, J = 7.1 Hz, 1H), 6.72−6.86 (m, 1H), 5.89 (d, J = 15.7 Hz, 1H), 5.32 (m, 1H), 4.55 (d, J = 12.4 Hz, 1H), 4.08−4.33 (m, 4H), 3.84 (m, 1H), 3.57 (d, J = 11.6 Hz, 1H), 2.96−3.15 (m, 1H), 2.59−2.76 (m, 1H), 1.44 (s, 9H), 1.29 (t, J = 6.6 Hz, 3H).

***tert*-Butyl 5-(4-Ethoxy-4-oxobutyl)-9-(*N*′-hydroxycarbamimidoyl)-2,3-dihydrobenzo[*f*][1,4]oxazepine-4(5*H*)-carboxylate (80).** Ethylenediamine (20 mL, 296 mmol) was added to a suspension of Pd/C (10% w/w, 50% wet, 10 g, 9.40 mmol) in EtOH (40 mL) under nitrogen, and the mixture was stirred for 16 h and then filtered, and the solid washed with EtOH (40 mL) and MTBE (40 mL). Compound **79** (92 g, 238 mmol) was dissolved in THF (400 mL) and was treated with activated charcoal (Norit, SC123792) for 1 h; then the solution was filtered through a filter cup and added to the solid palladium catalyst (10 g) under nitrogen. The vessel was purged, and the solution was hydrogenated at atmospheric pressure for 18 h. The expected hydrogen uptake was not achieved (only 800 mL consumed compared with expected approximately 6 L). The suspension was filtered under nitrogen and then added to fresh catalyst (8 g, prepared as above), giving very rapid hydrogen uptake. After 2 h, the mixture was filtered under nitrogen, and the filter pad was washed with EtOAc. The combined filtrates were evaporated *in vacuo* to give *tert*-butyl 9-cyano-5-(4-ethoxy-4-oxobutyl)-2,3-dihydrobenzo[*f*][1,4]oxazepine-4(5*H*)-carboxylate (92.5 g, 238 mmol, 100%) as a colorless oil, which crystallized on standing to a colorless crystalline solid. LCMS (method formate): retention time 1.20 min, $[M + H]^+$ = 389. ^1H NMR (250 MHz, DMSO-d_6) δ ppm 7.57 (m, 2H), 7.11−7.31 (m, 1H), 5.14 (t, J = 7.7 Hz, 1H), 4.49 (d, J = 12.3 Hz, 1H), 4.00−4.22 (m, 2H), 3.87 (t, J

dx.doi.org/10.1021/jm5010336 | J. Med. Chem. XXXX, XXX, XXX−XXX

= 10.7 Hz, 1H), 3.50−3.71 (m, 1H), 2.34 (t, J = 7.1 Hz, 2H), 2.05−2.21 (m, 1H), 1.56−1.92 (m, 4H), 1.41 (s, 9H), 1.21 (t, J = 6.9 Hz, 3H). A solution of this material (7.8 g, 20.08 mmol) in EtOH (40 mL) was treated with aqueous hydroxylamine (50% w/w, 10.6 g, 161 mmol), and the resulting mixture was stirred at reflux for 3 h and then cooled to room temperature and concentrated *in vacuo*. The residue was dried under vacuum at 40 °C for 16 h to give **80** (8.1 g, 19.22 mmol, 96%) as colorless gummy foam, which was used in the next step without further purification. LCMS (method formate): retention time 0.79 min, $[M + H]^+$ = 421. ^{1}H NMR (250 MHz, DMSO-d_6) δ ppm 8.94−9.06 (m, 1H), 7.33−7.44 (m, 1H), 7.17−7.26 (m, 1H), 6.97−7.09 (m, 1H), 5.33 (br s, 2H), 5.01−5.13 (m, 1H), 4.27−4.42 (m, 1H), 3.98−4.17 (m, 3H), 3.66−3.82 (m, 1H), 3.47−3.63 (m, 1H), 2.28−2.40 (m, 1 H), 2.06−2.24 (m, 1H), 1.73−1.90 (m, 1H), 1.46−1.69 (m, 1H), 1.38−1.44 (m, 2H), 1.43 (s, 9H), 1.21 (m, 3H).

***tert*-Butyl 9-(5-(5-Chloro-6-isopropoxypyridin-3-yl)-1,2,4-oxadiazol-3-yl)-5-(4-ethoxy-4-oxobutyl)-2,3-dihydrobenzo[*f*][1,4]oxazepine-4(5*H*)-carboxylate (81).** A mixture of 5-chloro-6-hydroxy-3-pyridinecarboxylic acid (13.85 g, 80 mmol), silver carbonate (44 g, 160 mmol), and 2-iodopropane (27.1 g, 160 mmol) in $CHCl_3$ (200 mL) was stirred at reflux for 3 days, and then was cooled to room temperature. The mixture was filtered through Celite and evaporated to give 1-methylethyl 5-chloro-6-[(1-methylethyl)oxy]-3-pyridinecarboxylate (16.44 g, 63.8 mmol, 80% yield) as a colorless liquid. LCMS (method formate): retention time 1.47 min, $[M + H]^+$ = 258. ^{1}H NMR (400 MHz, $CDCl_3$) δ ppm 8.69 (d, J = 2.3 Hz, 1H), 8.19 (d, J = 2.3 Hz, 1H), 5.45 (spt, J = 6.3 Hz, 1H), 5.25 (spt, J = 6.3 Hz, 1H), 1.42 (d, J = 6.3 Hz, 6H), 1.37 (d, J = 6.3 Hz, 6H. Sodium hydroxide (2 N in water, 63.5 mL, 127 mmol) was added to a solution of this material (16.4 g, 63.6 mmol) in EtOH (200 mL) at 0 °C, and the solution was then allowed to warm to room temperature and stirred for 1 h. Most of the solvent was evaporated *in vacuo*, and the aqueous residue was diluted with water and washed with Et_2O (100 mL) and then acidified with a 5 N HCl aqueous solution to pH 2. The precipitate was collected by filtration and dried under vacuum at 40 °C to give 5-chloro-6-[(1-methylethyl)oxy]-3-pyridinecarboxylic acid (13.3 g, 61.7 mmol, 97%) as a colorless solid. LCMS (method formate): retention time 1.05 min, $[M + H]^+$ = 214. ^{1}H NMR (250 MHz, DMSO-d_6) δ ppm 13.28 (br s, 1H), 8.65 (d, J = 2.0 Hz, 1H), 8.21 (d, J = 2.0 Hz, 1H), 5.41 (spt, J = 6.2 Hz, 1H), 1.36 (d, J = 6.2 Hz, 6H). Oxalyl chloride (12.18 mL, 139 mmol) was added to a suspension of this material (10g, 46.4 mmol) in CH_2Cl_2 (200 mL)m and the mixture was stirred at room temperature for 16 h. The solvent was then evaporated *in vacuo* to give 5-chloro-6-[(1-methylethyl)oxy]-3-pyridinecarbonyl chloride (10.7 g, 99%) as a yellow liquid. ^{1}H NMR (400 MHz, $CDCl_3$) δ ppm 8.82 (d, J = 2.3 Hz, 1H), 8.26 (d, J = 2.3 Hz, 1H), 5.51 (spt, J = 6.3 Hz, 1H), 1.45 (d, J = 6.3 Hz, 6H). A solution of this material (4.40 g, 18.8 mmol) in DMF (10 mL) was added to a solution of **80** (7.2 g, 17.1 mmol) and Et_3N (4.76 mL, 34.2 mmol) in DMF (80 mL) at room temperature. After 10 min, the resulting mixture was stirred at 80 °C for 1 h, then at 120 °C for 2 h, and then cooled to room temperature. The solution was diluted with water (600 mL) and then extracted with EtOAc (3 × 200 mL). The combined organic phases were washed with water (3 × 300 mL), dried over $MgSO_4$, and concentrated *in vacuo*. Purification of the residue by flash chromatography on silica gel (0−30% EtOAc in hexanes) gave racemic **81** (6.2 g, 60%) as a pale yellow oil. LCMS (method formate): retention time 1.61 min, $[M + H]^+$ = 602. ^{1}H NMR (400 MHz, DMSO-d_6) δ ppm 8.90 (d, J = 1.8 Hz, 1H), 8.47 (d, J = 1.8 Hz, 1H), 7.79 (d, J = 7.5 Hz, 1H), 7.46 (d, J = 7.3 Hz, 1H), 7.16−7.31 (m, 1H), 5.43−5.63 (m, 1H), 5.14 (br s, 1H), 4.41 (d, J = 12.5 Hz, 1H), 4.09 (q, J = 6.8 Hz, 3H), 3.79 (br s, 1H), 3.57−3.69 (m, 1H), 2.36 (t, J = 7.3 Hz, 2H), 2.15 (s, 1H), 1.80−1.95 (m, 1H), 1.58−1.73 (m, 1H), 1.34−1.55 (m, 16H), 1.21 (t, J = 7.0 Hz, 3H).

***tert*-Butyl 9-(5-(5-Chloro-6-isopropoxypyridin-3-yl)-1,2,4-oxadiazol-3-yl)-5-(4-ethoxy-4-oxobutyl)-2,3-dihydrobenzo[*f*][1,4]oxazepine-4(5*H*)-carboxylate Enantiomers (81a and 81b).** Analytical method: approximately 0.5 mg of racemic **81** was dissolved in 50/50 IPA/heptane (1 mL), 20 μL was injected on column; 10% IPA/heptane, f = 1.0 mL/min, wavelength 230 nm, ref 550,100, column 4.6 mm id × 25 cm Chiralpak AS, lot no. AS00CE-J040. Preparative method: approximately 600 mg of racemic **81** was dissolved in 2 mL of IPA and 2 mL of heptane, and the solution was injected onto the column; 10% IPA/heptane, f = 75 mL/min, wavelength 260 nm, ref 550,100, column 5 cm × 20 cm Chiralpak AS (20 um) self-packed, total number of injections 2. Fraction collection: Fractions from 7 to 10 min were combined and labeled isomer 1. Fractions from 12 to 30 min were combined and labeled isomer 2. Both combined fractions of isomers 1 and 2 were then concentrated using a rotary evaporator and transferred to weighed flasks for final analysis as described by the analytical method above. Isomer 1, 450 mg; isomer 2, 465 mg. LCMS (method formate): retention time 1.61 min, $[M + H]^+$ = 602. ^{1}H NMR (400 MHz, DMSO-d_6) δ ppm 8.90 (d, J = 1.8 Hz, 1H), 8.47 (d, J = 1.8 Hz, 1H), 7.79 (d, J = 7.5 Hz, 1H), 7.46 (d, J = 7.3 Hz, 1H), 7.16−7.31 (m, 1H), 5.43−5.63 (m, 1H), 5.14 (br s, 1H), 4.41 (d, J = 12.5 Hz, 1H), 4.09 (q, J = 6.8 Hz, 3H), 3.79 (br s, 1H), 3.57−3.69 (m, 1H), 2.36 (t, J = 7.3 Hz, 2H), 2.15 (s, 1H), 1.80−1.95 (m, 1H), 1.58−1.73 (m, 1H), 1.34−1.55 (m, 16H), 1.21 (t, J = 7.0 Hz, 3H).

4-(9-(5-(5-Chloro-6-isopropoxypyridin-3-yl)-1,2,4-oxadiazol-3-yl)-2,3,4,5-tetrahydrobenzo[*f*][1,4]oxazepin-5-yl)butanoic Acid Hydrochloride Enantiomers (31a and 31b). This procedure was used for each enantiomer separately. A suspension of **81a** (450 mg, 0.75 mmol) in EtOH (2 mL) was treated with a 2 N NaOH aqueous solution (2 mL), and the resulting mixture was stirred at 50 °C for 2 h and then was cooled to room temperature. Most of the EtOH was removed *in vacuo*, and the residue was diluted with water and acidified with glacial acetic acid. The mixture was extracted with EtOAc (2 × 10 mL). The combined organic phases were dried over $MgSO_4$ and concentrated *in vacuo* to give 4-(4-(*tert*-butoxycarbonyl)-9-(5-(5-chloro-6-isopropoxypyridin-3-yl)-1,2,4-oxadiazol-3-yl)-2,3,4,5-tetrahydrobenzo[*f*][1,4]oxazepin-5-yl)butanoic acid (398 mg, 93%) as a colorless crispy foam. LCMS (method High pH): retention time 1.17 min, $[M + H]^+$ = 573. ^{1}H NMR (400 MHz, DMSO-d_6) δ ppm 11.89−12.34 (m, 1H), 8.92 (d, J = 2.3 Hz, 1H), 8.54 (d, J = 2.0 Hz, 1H), 7.79 (d, J = 6.8 Hz, 1H), 7.38−7.57 (m, 1H), 7.27 (br s, 1H), 5.35−5.58 (m, 1H), 4.92−5.26 (m, 1H), 4.33−4.56 (m, 1H), 3.94−4.16 (m, 1H), 3.65 (br s, 2H), 2.28 (m., 3H), 1.71−1.84 (m, 1H), 1.48−1.64 (m, 1H), 1.29−1.45 (m, 16H). A solution of this material (390 mg, 0.68 mmol) in 1,4-dioxane (3 mL) was treated with HCl (4 N in 1,4-dioxane, 2 mL, 8 mmol), and the resulting mixture was stirred at room temperature for 3 h. Et_2O (25 mL) was added, and the mixture was stirred for 30 min. The solid formed was filtered off, washed with Et_2O, and dried under vacuum to give 4-(9-(5-(5-chloro-6-isopropoxypyridin-3-yl)-1,2,4-oxadiazol-3-yl)-2,3,4,5-tetrahydrobenzo[f][1,4]oxazepin-5-yl)butanoic acid hydrochloride (263 mg, 76%) as a white solid. Compound **31a** is the fast running enantiomer, and compound **31b** is the slow running enantiomer. LCMS (method high pH): retention time 0.97 min, $[M + H]^+$ = 473. ^{1}H NMR (400 MHz, DMSO-d_6) δ ppm 8.58−8.72 (m, 2H), 8.51 (d, J = 2.0 Hz, 1H), 8.40 (dd, J = 8.8, 2.3 Hz, 1H), 7.69−7.81 (m, 1H), 7.56 (d, J = 9.1 Hz, 1H), 7.19−7.37 (m, 1H), 5.28 (d, J = 5.1 Hz, 2H), 4.99 (s, 1H), 4.75 (d, J = 18.7 Hz, 2H), 4.24 (br s, 2H), 3.60−3.76 (m, 2H), 3.17−3.29 (m, 2H), 2.94 (m., 2H), 1.33−1.46 (m, 6H).

S1P$_1$ and S1P$_3$ Receptor GTPγS Assays. Receptor assays were performed as described previously.[26] Briefly, homogenized S1P$_1$-expressing RH7777 membranes or S1P$_3$-expressing RBL membranes were adhered to WGA-coated SPA beads in assay buffer. After 30 min precoupling on ice, the bead and membrane suspension was dispensed into white Greiner polypropylene LV 384-well plates (5 μL/well) containing 0.1 μL of compound. [^{35}S]-GTPγS (5 μL/well, 0.5 nM for S1P$_1$ or 0.3 nM for S1P$_3$ final radioligand concentration) made in assay buffer was then added to the plates. The final assay cocktail was then sealed, spun on a centrifuge, and then read immediately on a Viewlux instrument.

Rat Lymphocyte Reduction Studies. This procedure was performed as described previously.[26] Briefly, male Lewis rats had predose blood samples (200 μL) removed by direct venipuncture the day prior to oral dosing. On the study day, rats (n = 4 per group) received either vehicle (1% methycellulose 4 mL/kg po) or compound

dx.doi.org/10.1021/jm5010336 | J. Med. Chem. XXXX, XXX, XXX−XXX

(0.1−3 mg/kg po) and had further blood samples taken at 0.25, 0.5, 1, 2, 4, 7, 12, 24, 30, 36, 48, and 54 h postdose. From each blood sample, 50 μL was mixed with 50 μL of water for pharmacokinetic analysis. The remainder of the blood samples were analyzed using the Sysmex XT2000iV automatic hematology analyzer for lymphocyte counts.

■ ASSOCIATED CONTENT

Supporting Information

Experimental procedures for the synthesis of compounds **8**−**30**, in vitro assay protocols for the determination of EC_{50}, and protocols for *in vivo* studies and data correlations. This material is available free of charge via the Internet at http://pubs.acs.org.

■ AUTHOR INFORMATION

Corresponding Authors

*E.D. Tel: +44 1438 764319. Fax: +44 1438 768302. E-mail: emmanuel.h.demont@gsk.com.

*T.D.H. Tel: +44 1223 226200. Fax: +44 1223 226201. E-mail: tom.heightman@astx.com.

Author Contributions

The manuscript was written through contributions of all authors. All authors have given approval to the final version of the manuscript. J. Skidmore and J. Heer contributed equally.

Notes

The authors declare no competing financial interest.

■ ACKNOWLEDGMENTS

The authors thank Mr Nigel Quashie, Miss Sapna Desai, Miss Sandra Arpino, and Miss Jenni Cryan for assay support, Dr. Richard Upton and Mr. Nick Waite for NMR support, Dr. Bill Leavens for recording HRMS spectra, Mrs. Helen Tracey for conducting permeability experiments, Mrs. Catherine Cartwright, and Miss Aarti Patel for determining intrinsic clearance, Mr. Nigel Deeks, Mr. Rob Willis, Mr. James Gray, and Miss Tingting Fu for generation of the in vivo DMPK data, and Dr. Colin Campbell, Miss Pam Gaskin, and Mrs. Karen Leavens for supporting the lymphopenia studies. Mrs. Shenaz Nunhuck and Mr. Alan Hill are also acknowledged for pK_a and CHI determination, and Miss Helen Garden is acknowledged for solubility measurements.

■ ABBREVIATIONS

CHI, chromatographic hydrophobicity index; DMF, dimethylformamide; DMS, dimethylsulfide; EDC, 1-ethyl-3-(3-(dimethylamino)propyl) carbodiimide; F_{ub}, unbound fraction; HOBt, hydroxybenzotriazole; HSA, human serum albumin; LDA, lithium diisopropyl amide; MDCK, Madin−Darby canine kidney; NBS, *N*-bromosuccinimide; PD, pharmacodynamic; PK, pharmacokinetic; TFA, trifluoroacetic acid; THF, tetrahydrofuran; THIQ, tetrahydroisoquinoline

■ REFERENCES

(1) Singer, B.; Ross, A. P.; Tobias, K. Oral fingolimod for the treatment of patients with relapsing forms of multiple sclerosis. *Int. J. Clin. Pract.* **2011**, *65*, 887−895.

(2) Fujino, M.; Funeshima, N.; Kitazawa, Y.; Kimura, H.; Amemiya, H.; Suzuki, S.; Li, X.-K. Amelioration of Experimental Autoimmune Encephalomyelitis in Lewis Rats by FTY720 Treatment. *J. Pharmacol. Exp. Ther.* **2003**, *305*, 70−77.

(3) Comi, G.; O'Connor, P.; Montalban, X.; Antel, J.; Radue, E.-W.; Karlsson, G.; Pohlmann, H.; Aradhye, S.; Kappos, L.; FTY720D2201 Study Group. Phase II study of oral fingolimod (FTY720) in multiple sclerosis: 3-year results. *Mult. Scler.* **2010**, *16*, 197−207.

(4) Billich, A.; Bornancin, F.; Dévay, P.; Mechtcheriakova, D.; Urtz, N.; Baumruker, T. Phosphorylation of the Immunomodulatory Drug FTY720 by Sphingosine Kinases. *J. Biol. Chem.* **2003**, *278*, 47408−47415.

(5) Albert, R.; Hinterding, K.; Brinkmann, V.; Guerini, D.; Müller-Hartwieg, C.; Knecht, H.; Simeon, C.; Streiff, M.; Wagner, T.; Welzenbach, K.; Zécri, F.; Zollinger, M.; Cooke, N.; Francotte, E. Novel Immunomodulator FTY720 Is Phosphorylated in Rats and Humans To Form a Single Stereoisomer. Identification, Chemical Proof, and Biological Characterization of the Biologically Active Species and Its Enantiomer. *J. Med. Chem.* **2005**, *48*, 5373−5377.

(6) Adachi, K.; Chiba, K. FTY720 Story. Its Discovery and the Following Accelerated Development of Sphingosine 1-Phosphate Receptor Agonists as Immunomodulators Based on Reverse Pharmacology. *Perspect. Med. Chem.* **2007**, *1*, 11.

(7) Matloubian, M.; Lo, C. G.; Cinamon, G.; Lesneski, M. J.; Xu, Y.; Brinkmann, V.; Allende, M. L.; Proia, R. L.; Cyster, J. G. Lymphocyte egress from thymus and peripheral lymphoid organs is dependent on S1P receptor 1. *Nature* **2004**, *427*, 355−360.

(8) Wei, S. H.; Rosen, H.; Matheu, M. P.; Sanna, M. G.; Wang, S.-K.; Jo, E.; Wong, C.-H.; Parker, I.; Cahalan, M. D. Sphingosine 1-phosphate type 1 receptor agonism inhibits transendothelial migration of medullary T cells to lymphatic sinuses. *Nat. Immunol.* **2005**, *6*, 1228−1235.

(9) Choi, J. W.; Gardell, S. E.; Herr, D. R.; Rivera, R.; Lee, C.-W.; Noguchi, K.; Teo, S. T.; Yung, Y. C.; Lu, M.; Kennedy, G.; Chun, J. FTY720 (fingolimod) efficacy in an animal model of multiple sclerosis requires astrocyte sphingosine 1-phosphate receptor 1 (S1P1) modulation. *Proc. Natl. Acad. Sci. U. S. A.* **2011**, *108*, 751−756.

(10) Cohen, J. A.; Chun, J. Mechanisms of fingolimod's efficacy and adverse effects in multiple sclerosis. *Ann. Neurol.* **2011**, *69*, 759−777.

(11) Forrest, M.; Sun, S.-Y.; Hajdu, R.; Bergstrom, J.; Card, D.; Doherty, G.; Hale, J.; Keohane, C.; Meyers, C.; Milligan, J.; Mills, S.; Nomura, N.; Rosen, H.; Rosenbach, M.; Shei, G.-J.; Singer, I. I.; Tian, M.; West, S.; White, V.; Xie, J.; Proia, R. L.; Mandala, S. Immune Cell Regulation and Cardiovascular Effects of Sphingosine 1-Phosphate Receptor Agonists in Rodents Are Mediated via Distinct Receptor Subtypes. *J. Pharmacol. Exp. Ther.* **2004**, *309*, 758−768.

(12) Sanna, M. G.; Liao, J.; Jo, E.; Alfonso, C.; Ahn, M.-Y.; Peterson, M. S.; Webb, B.; Lefebvre, S.; Chun, J.; Gray, N.; Rosen, H. Sphingosine 1-Phosphate (S1P) Receptor Subtypes S1P1 and S1P3, Respectively, Regulate Lymphocyte Recirculation and Heart Rate. *J. Biol. Chem.* **2004**, *279*, 13839−13848.

(13) Gergely, P.; Wallström, E.; Nuesslein-Hildesheim, B.; Bruns, C.; Zécri, F.; Cooke, N.; Traebert, M.; Tuntland, T.; Rosenberg, M.; Saltzman, M. Phase I study with the selective S1P1/S1P5 receptor modulator BAF312 indicates that S1P1 rather than S1P3 mediates transient heart rate reduction in humans. *Mult. Scler.* **2009**, *15*, S235−S236.

(14) Bolli, M.; Lescop, C.; Nayler, O. Synthetic Sphingosine 1-Phosphate Receptor Modulators - Opportunities and Potential Pitfalls. *Curr. Top. Med. Chem.* **2011**, *11*, 726−757.

(15) Evindar, G.; Bernier, S. G.; Doyle, E.; Kavarana, M. J.; Satz, A. L.; Lorusso, J.; Blanchette, H. S.; Saha, A. K.; Hannig, G.; Morgan, B. A.; Westlin, W. F. Exploration of amino alcohol derivatives as novel, potent, and highly selective sphingosine-1-phosphate receptor subtype-1 agonists. *Bioorg. Med. Chem. Lett.* **2010**, *20*, 2520−2524.

(16) Vachal, P.; Toth, L. M.; Hale, J. J.; Yan, L.; Mills, S. G.; Chrebet, G. L.; Koehane, C. A.; Hajdu, R.; Milligan, J. A.; Rosenbach, M. J.; Mandala, S. Highly selective and potent agonists of sphingosine-1-phosphate 1 (S1P1) receptor. *Bioorg. Med. Chem. Lett.* **2006**, *16*, 3684−3687.

(17) Hale, J. J.; Lynch, C. L.; Neway, W.; Mills, S. G.; Hajdu, R.; Keohane, C. A.; Rosenbach, M. J.; Milligan, J. A.; Shei, G.-J.; Parent, S. A.; Chrebet, G.; Bergstrom, J.; Card, D.; Ferrer, M.; Hodder, P.; Strulovici, B.; Rosen, H.; Mandala, S. A Rational Utilization of High-Throughput Screening Affords Selective, Orally Bioavailable 1-Benzyl-3-carboxyazetidine Sphingosine-1-phosphate-1 Receptor Agonists. *J. Med. Chem.* **2004**, *47*, 6662−6665.

(18) Piali, L.; Froidevaux, S.; Hess, P.; Nayler, O.; Bolli, M. H.; Schlosser, E.; Kohl, C.; Steiner, B.; Clozel, M. The Selective Sphingosine 1-Phosphate Receptor 1 Agonist Ponesimod Protects against Lymphocyte-Mediated Tissue Inflammation. *J. Pharmacol. Exp. Ther.* **2011**, *337*, 547−556.
(19) Pelletier, D.; Hafler, D. A. Fingolimod for Multiple Sclerosis. *New Engl. J. Med.* **2012**, *366*, 339−347.
(20) David, O. J.; Kovarik, J. M.; Schmouder, R. L. Clinical Pharmacokinetics of Fingolimod. *Clin. Pharmacokinet.* **2012**, *51*, 15−28.
(21) Montanari, D.; Chiarparin, E.; Gleeson, M. P.; Braggio, S.; Longhi, R.; Valko, K.; Rossi, T. Application of drug efficiency index in drug discovery: a strategy towards low therapeutic dose. *Exp. Opin. Drug Discovery* **2011**, *6*, 913−920.
(22) Leeson, P. D.; St-Gallay, S. A. The influence of the 'organizational factor' on compound quality in drug discovery. *Nat. Rev. Drug Discovery* **2011**, *10*, 749−765.
(23) Hughes, J. D.; Blagg, J.; Price, D. A.; Bailey, S.; DeCrescenzo, G. A.; Devraj, R. V.; Ellsworth, E.; Fobian, Y. M.; Gibbs, M. E.; Gilles, R. W.; Greene, N.; Huang, E.; Krieger-Burke, T.; Loesel, J.; Wager, T.; Whiteley, L.; Zhang, Y. Physiochemical drug properties associated with in vivo toxicological outcomes. *Bioorg. Med. Chem. Lett.* **2008**, *18*, 4872−4875.
(24) McKeown, S. C.; Hall, A.; Giblin, G. M. P.; Lorthioir, O.; Blunt, R.; Lewell, X. Q.; Wilson, R. J.; Brown, S. H.; Chowdhury, A.; Coleman, T.; Watson, S. P.; Chessell, I. P.; Pipe, A.; Clayton, N.; Goldsmith, P. Identification of novel pyrazole acid antagonists for the EP1 receptor. *Bioorg. Med. Chem. Lett.* **2006**, *16*, 4767−4771.
(25) Li, Z.; Chen, W.; Hale, J. J.; Lynch, C. L.; Mills, S. G.; Hajdu, R.; Keohane, C. A.; Rosenbach, M. J.; Milligan, J. A.; Shei, G.-J.; Chrebet, G.; Parent, S. A.; Bergstrom, J.; Card, D.; Forrest, M.; Quackenbush, E. J.; Wickham, L. A.; Vargas, H.; Evans, R. M.; Rosen, H.; Mandala, S. Discovery of Potent 3,5-Diphenyl-1,2,4-oxadiazole Sphingosine-1-phosphate-1 (S1P1) Receptor Agonists with Exceptional Selectivity against S1P2 and S1P3. *J. Med. Chem.* **2005**, *48*, 6169−6173.
(26) Demont, E. H.; Arpino, S.; Bit, R. A.; Campbell, C. A.; Deeks, N.; Desai, S.; Dowell, S. J.; Gaskin, P.; Gray, J. R. J.; Harrison, L. A.; Haynes, A.; Heightman, T. D.; Holmes, D. S.; Humphreys, P. G.; Kumar, U.; Morse, M. A.; Osborne, G. J.; Panchal, T.; Philpott, K. L.; Taylor, S.; Watson, R.; Willis, R.; Witherington, J. Discovery of a Brain-Penetrant S1P3-Sparing Direct Agonist of the S1P1 and S1P5 Receptors Efficacious at Low Oral Dose. *J. Med. Chem.* **2011**, *54*, 6724−6733.
(27) Beaudry, F.; Coutu, M.; Brown, N. K. Determination of drug−plasma protein binding using human serum albumin chromatographic column and multiple linear regression model. *Biomed. Chromatogr.* **1999**, *13*, 401−406.
(28) Roberts, M.; Magnusson, B.; Burczynski, F.; Weiss, M. Enterohepatic Circulation. *Clin. Pharmacokinet.* **2002**, *41*, 751−790.
(29) Yan, L.; Huo, P.; Doherty, G.; Toth, L.; Hale, J. J.; Mills, S. G.; Hajdu, R.; Keohane, C. A.; Rosenbach, M. J.; Milligan, J. A.; Shei, G.-J.; Chrebet, G.; Bergstrom, J.; Card, D.; Quackenbush, E.; Wickham, A.; Mandala, S. M. Discovery of 3-arylpropionic acids as potent agonists of sphingosine-1-phosphate receptor-1 (S1P1) with high selectivity against all other known S1P receptor subtypes. *Bioorg. Med. Chem. Lett.* **2006**, *16*, 3679−3683.
(30) Cahalan, S. M.; Gonzalez-Cabrera, P. J.; Sarkisyan, G.; Nguyen, N.; Schaeffer, M.-T.; Huang, L.; Yeager, A.; Clemons, B.; Scott, F.; Rosen, H. Actions of a picomolar short-acting S1P1 agonist in S1P1-eGFP knock-in mice. *Nat. Chem. Biol.* **2011**, *7*, 254−256.
(31) Nicolaides, E.; Galia, E.; Efthymiopoulos, C.; Dressman, J. B.; Reppas, C. Forecasting the In Vivo Performance of Four Low Solubility Drugs from Their In Vitro Dissolution Data. *Pharm. Res.* **1999**, *16*, 1876−1882.
(32) Taylor, S.; Gray, J. R. J.; Willis, R.; Deeks, N.; Haynes, A.; Campbell, C.; Gaskin, P.; Leavens, K.; Demont, E.; Dowell, S.; Cryan, J.; Morse, M.; Patel, A.; Garden, H.; Witherington, J. The utility of pharmacokinetic−pharmacodynamic modeling in the discovery and optimization of selective S1P1 agonists. *Xenobiotica* **2012**, *42*, 671.
(33) Gleeson, M. P.; Hersey, A.; Montanari, D.; Overington, J. Probing the links between in vitro potency, ADMET and physicochemical parameters. *Nat. Rev. Drug Discovery* **2011**, *10*, 197−208.
(34) Jones, L. H.; Summerhill, N. W.; Swain, N. A.; Mills, J. E. Aromatic chloride to nitrile transformation: medicinal and synthetic chemistry. *Med. Chem. Commun.* **2010**, *1*, 309−318.
(35) Fleming, F. F.; Yao, L.; Ravikumar, P. C.; Funk, L.; Shook, B. C. Nitrile-Containing Pharmaceuticals: Efficacious Roles of the Nitrile Pharmacophore. *J. Med. Chem.* **2010**, *53*, 7902−7917.
(36) Lovering, F.; Bikker, J.; Humblet, C. Escape from Flatland: Increasing Saturation as an Approach to Improving Clinical Success. *J. Med. Chem.* **2009**, *52*, 6752−6756.
(37) Schürer, S. C.; Brown, S. J.; Gonzalez-Cabrera, P. J.; Schaeffer, M.-T.; Chapman, J.; Jo, E.; Chase, P.; Spicer, T.; Hodder, P.; Rosen, H. Ligand-Binding Pocket Shape Differences between Sphingosine 1-Phosphate (S1P) Receptors S1P1 and S1P3 Determine Efficiency of Chemical Probe Identification by Ultrahigh-Throughput Screening. *ACS Chem. Biol.* **2008**, *3*, 486−498.
(38) Valkó, K.; Bevan, C.; Reynolds, D. Chromatographic Hydrophobicity Index by Fast-Gradient RP-HPLC: A High-Throughput Alternative to log P/log D. *Anal. Chem.* **1997**, *69*, 2022−2029.
(39) Skidmore, J.; Atcha, Z.; Boucherat, E.; Castelletti, L.; Chen, D. W.; Coppo, F. T.; Cutler, L.; Dunsdon, R. M.; Heath, B. M.; Hutchings, R.; Hurst, D. N.; Javed, S.; Martin, S.; Maskell, E. S. L.; Norton, D.; Pemberton, D. J.; Redshaw, S.; Rutter, R.; Sehmi, S. S.; Scoccitti, T.; Temple, H. E.; Theobald, P.; Ward, R. W.; Wilson, D. M. The discovery of 2-fluoro-N-(3-fluoro-4-(5-((4-morpholinobutyl)-amino)-1,3,4-oxadiazol-2-yl)phenyl) benzamide, a full agonist of the alpha-7 nicotinic acetylcholine receptor showing efficacy in the novel object recognition model of cognition enhancement. *Bioorg. Med. Chem. Lett.* **2012**, *22*, 3531−3534.
(40) Wang, Q.; Rager, J. D.; Weinstein, K.; Kardos, P. S.; Dobson, G. L.; Li, J.; Hidalgo, I. J. Evaluation of the MDR-MDCK cell line as a permeability screen for the blood−brain barrier. *Int. J. Pharmaceut.* **2005**, *288*, 349−359.
(41) Further analysis showed that one of the four rats used in the 1 mg/kg study for compound **31a** had a significantly prolonged lymphopenia compared with the other three rats, hence the average prolonged effect. See Experimental Section for details.
(42) Bonanomi, G.; Cardullo, F.; Damiani, F.; Gentile, G.; Hamprecht, D.; Micheli, F.; Tarsi, L. (Glaxo Group Limited, U.K.) Preparation of fused benzazepines having affinity for the dopamine D3 receptor. Int. Patent Appl. WO2006002928, 12 Jan 2006.